9. Shembade N, Harhaj NS, Liebl DJ, Harhaj EW (2007) Essential role for TAX1BP1 in the termination of TNF-alpha-, IL-1- and LPS-mediated NF-kappaB and JNK signaling. EMBO J 26: 3910–3922.
10. Ling L, Goeddel DV (2000) T6BP, a TRAF6-interacting protein involved in IL-1 signaling. Proc Natl Acad Sci U S A 97: 9567–9572.
11. Peloponese JM, Yeung ML, Jeang KT (2006) Modulation of nuclear factor-kappaB by human T cell leukemia virus type 1 Tax protein: implications for oncogenesis and inflammation. Immunol Res 34: 1–12.
12. Giam CZ, Jeang KT (2007) HTLV-1 Tax and adult T-cell leukemia. Front Biosci 12: 1496–1507.
13. Shembade N, Harhaj NS, Parvatiyar K, Copeland NG, Jenkins NA, et al. (2008) The E3 ligase Itch negatively regulates inflammatory signaling pathways by controlling the function of the ubiquitin-editing enzyme A20. Nat Immunol 9: 254–262.
14. Verstrepen L, Verhelst K, Carpentier I, Beyaert R (2011) TAX1BP1, a ubiquitin-binding adaptor protein in innate immunity and beyond. Trends Biochem Sci 36: 347–354.
15. Yamaoka S, Courtois G, Bessia C, Whiteside ST, Weil R, et al. (1998) Complementation cloning of NEMO, a component of the IkappaB kinase complex essential for NF-kappaB activation. Cell 93: 1231–1240.
16. Hida A, Imaizumi M, Sera N, Akahoshi M, Soda M, et al. (2010) Association of human T lymphotropic virus type I with Sjogren syndrome. Ann Rheum Dis 69: 2056–2057.
17. Kira J, Hamada T, Kawano Y, Okayama M, Yamasaki K (1997) An association of human T-cell lymphotropic virus type I infection with vascular dementia. Acta Neurol Scand 96: 305–309.
18. Hayashi J, Furusyo N, Sawayama Y, Murata M (2008) [Chronic infection is one of the etiologies for digestive diseases and atherosclerosis]. Fukuoka Igaku Zasshi 99: 67–73.
19. Vereecke L, Beyaert R, van Loo G (2009) The ubiquitin-editing enzyme A20 (TNFAIP3) is a central regulator of immunopathology. Trends Immunol 30: 383–391.
20. Kawai T, Adachi O, Ogawa T, Takeda K, Akira S (1999) Unresponsiveness of MyD88-deficient mice to endotoxin. Immunity 11: 115–122.
21. Sadanaga A, Nakashima H, Akahoshi M, Masutani K, Miyake K, et al. (2007) Protection against autoimmune nephritis in MyD88-deficient MRL/lpr mice. Arthritis Rheum 56: 1618–1628.
22. Benjamini Y, Drai D, Elmer G, Kafkafi N, Golani I (2001) Controlling the false discovery rate in behavior genetics research. Behav Brain Res 125: 279–284.
23. Iha H, Kibler KV, Yedavalli VR, Peloponese JM, Haller K, et al. (2003) Segregation of NF-kappaB activation through NEMO/IKKgamma by Tax and TNFalpha: implications for stimulus-specific interruption of oncogenic signaling. Oncogene 22: 8912–8923.
24. Rakoff-Nahoum S, Paglino J, Eslami-Varzaneh F, Edberg S, Medzhitov R (2004) Recognition of commensal microflora by toll-like receptors is required for intestinal homeostasis. Cell 118: 229–241.
25. Obici L, Merlini G (2012) Amyloidosis in autoinflammatory syndromes. Autoimmun Rev 12: 14–17.
26. Jang SY, Shin YK, Lee HY, Park JY, Suh DJ, et al. (2012) Local production of serum amyloid a is implicated in the induction of macrophage chemoattractants in Schwann cells during wallerian degeneration of peripheral nerves. Glia 60: 1619–1628.
27. Poynter ME (2012) Airway epithelial regulation of allergic sensitization in asthma. Pulm Pharmacol Ther 25: 438–446.
28. Geijtenbeek TB, Gringhuis SI (2009) Signalling through C-type lectin receptors: shaping immune responses. Nat Rev Immunol 9: 465–479.
29. Kapoor M, Martel-Pelletier J, Lajeunesse D, Pelletier JP, Fahmi H (2011) Role of proinflammatory cytokines in the pathophysiology of osteoarthritis. Nat Rev Rheumatol 7: 33–42.
30. Goldszmid RS, Trinchieri G (2012) The price of immunity. Nat Immunol 13: 932–938.
31. Lee CG, Da Silva CA, Dela Cruz CS, Ahangari F, Ma B, et al. (2011) Role of chitin and chitinase/chitinase-like proteins in inflammation, tissue remodeling, and injury. Annu Rev Physiol 73: 479–501.
32. Das R, Philip S, Mahabeleshwar GH, Bulbule A, Kundu GC (2005) Osteopontin: it's role in regulation of cell motility and nuclear factor kappa B-mediated urokinase type plasminogen activator expression. IUBMB Life 57: 441–447.
33. Gudjonsson JE, Johnston A, Stoll SW, Riblett MB, Xing X, et al. (2010) Evidence for altered Wnt signaling in psoriatic skin. J Invest Dermatol 130: 1849–1859.
34. Chien AJ, Conrad WH, Moon RT (2009) A Wnt survival guide: from flies to human disease. J Invest Dermatol 129: 1614–1627.
35. Surmann-Schmitt C, Dietz U, Kireva T, Adam N, Park J, et al. (2008) Ucma, a novel secreted cartilage-specific protein with implications in osteogenesis. J Biol Chem 283: 7082–7093.
36. Heineke J, Auger-Messier M, Correll RN, Xu J, Benard MJ, et al. (2010) CIB1 is a regulator of pathological cardiac hypertrophy. Nat Med 16: 872–879.
37. Berrebi D, Bruscoli S, Cohen N, Foussat A, Migliorati G, et al. (2003) Synthesis of glucocorticoid-induced leucine zipper (GILZ) by macrophages: an anti-inflammatory and immunosuppressive mechanism shared by glucocorticoids and IL-10. Blood 101: 729–738.
38. Wilson W, Taubert KA, Gewitz M, Lockhart PB, Baddour LM, et al. (2008) Prevention of infective endocarditis: guidelines from the American Heart Association: a guideline from the American Heart Association Rheumatic Fever, Endocarditis and Kawasaki Disease Committee, Council on Cardiovascular Disease in the Young, and the Council on Clinical Cardiology, Council on Cardiovascular Surgery and Anesthesia, and the Quality of Care and Outcomes Research Interdisciplinary Working Group. J Am Dent Assoc 139 Suppl: 3S–24S.
39. Sandler NG, Douek DC (2012) Microbial translocation in HIV infection: causes, consequences and treatment opportunities. Nat Rev Microbiol 10: 655–666.
40. Tattermusch S, Bangham CR (2012) HTLV-1 infection: what determines the risk of inflammatory disease? Trends Microbiol 20: 494–500.
41. Martin F, Taylor GP (2011) Prospects for the management of human T-cell lymphotropic virus type 1-associated myelopathy. AIDS Rev 13: 161–170.
42. Yagi H, Takigawa M, Hashizume H (2003) Cutaneous type of adult T cell leukemia/lymphoma: a new entity among cutaneous lymphomas. J Dermatol 30: 641–643.
43. Uhlar CM, Whitehead AS (1999) Serum amyloid A, the major vertebrate acute-phase reactant. Eur J Biochem 265: 501–523.
44. Elias JA, Homer RJ, Hamid Q, Lee CG (2005) Chitinases and chitinase-like proteins in T(H)2 inflammation and asthma. J Allergy Clin Immunol 116: 497–500.
45. Quaye IK (2008) Haptoglobin, inflammation and disease. Trans R Soc Trop Med Hyg 102: 735–742.
46. Dinarello CA (2009) Immunological and inflammatory functions of the interleukin-1 family. Annu Rev Immunol 27: 519–550.
47. Uede T (2011) Osteopontin, intrinsic tissue regulator of intractable inflammatory diseases. Pathol Int 61: 265–280.
48. Iwakura Y, Tosu M, Yoshida E, Takiguchi M, Sato K, et al. (1991) Induction of inflammatory arthropathy resembling rheumatoid arthritis in mice transgenic for HTLV-I. Science 253: 1026–1028.
49. Green JE, Hinrichs SH, Vogel J, Jay G (1989) Exocrinopathy resembling Sjogren's syndrome in HTLV-1 tax transgenic mice. Nature 341: 72–74.
50. Ishiguro N, Abe M, Seto K, Sakurai H, Ikeda H, et al. (1992) A rat model of human T lymphocyte virus type I (HTLV-I) infection. 1. Humoral antibody response, provirus integration, and HTLV-I-associated myelopathy/tropical spastic paraparesis-like myelopathy in seronegative HTLV-I carrier rats. J Exp Med 176: 981–989.
51. Hasegawa H, Sawa H, Lewis MJ, Orba Y, Sheehy N, et al. (2006) Thymus-derived leukemia-lymphoma in mice transgenic for the Tax gene of human T-lymphotropic virus type I. Nat Med 12: 466–472.
52. Ohsugi T, Kumasaka T, Okada S, Urano T (2007) The Tax protein of HTLV-1 promotes oncogenesis in not only immature T cells but also mature T cells. Nat Med 13: 527–528.
53. Dewan MZ, Terashima K, Taruishi M, Hasegawa H, Ito M, et al. (2003) Rapid tumor formation of human T-cell leukemia virus type 1-infected cell lines in novel NOD-SCID/gammac(null) mice: suppression by an inhibitor against NF-kappaB. J Virol 77: 5286–5294.
54. Chervonsky AV (2010) Influence of microbial environment on autoimmunity. Nat Immunol 11: 28–35.
55. Gould FK, Denning DW, Elliott TS, Foweraker J, Perry JD, et al. (2012) Guidelines for the diagnosis and antibiotic treatment of endocarditis in adults: a report of the Working Party of the British Society for Antimicrobial Chemotherapy. J Antimicrob Chemother 67: 269–289.
56. Seckeler MD, Hoke TR (2011) The worldwide epidemiology of acute rheumatic fever and rheumatic heart disease. Clin Epidemiol 3: 67–84.
57. Chu VH, Woods CW, Miro JM, Hoen B, Cabell CH, et al. (2008) Emergence of coagulase-negative staphylococci as a cause of native valve endocarditis. Clin Infect Dis 46: 232–242.
58. Moreillon P, Que YA (2004) Infective endocarditis. Lancet 363: 139–149.
59. Oliere S, Douville R, Sze A, Belgnaoui SM, Hiscott J (2011) Modulation of innate immune responses during human T-cell leukemia virus (HTLV-1) pathogenesis. Cytokine Growth Factor Rev 22: 197–210.
60. Roufosse FE, Goldman M, Cogan E (2007) Hypereosinophilic syndromes. Orphanet J Rare Dis 2: 37.
61. Musone SL, Taylor KE, Lu TT, Nititham J, Ferreira RC, et al. (2008) Multiple polymorphisms in the TNFAIP3 region are independently associated with systemic lupus erythematosus. Nat Genet 40: 1062–1064.
62. Matmati M, Jacques P, Maelfait J, Verheugen E, Kool M, et al. (2011) A20 (TNFAIP3) deficiency in myeloid cells triggers erosive polyarthritis resembling rheumatoid arthritis. Nat Genet 43: 908–912.
63. Sartelet A, Druet T, Michaux C, Fasquelle C, Geron S, et al. (2012) A splice site variant in the bovine RNF11 gene compromises growth and regulation of the inflammatory response. PLoS Genet 8: e1002581.
64. Ruiz MT, Balachi JF, Fernandes RA, Galbiatti AL, Maniglia JV, et al. (2010) Analysis of the TAX1BP1 gene in head and neck cancer patients. Braz J Otorhinolaryngol 76: 193–198.

Available online at www.sciencedirect.com

SciVerse ScienceDirect

Journal of Nutritional Biochemistry 24 (2013) 256–266

Journal of Nutritional Biochemistry

Prenatal zinc deficiency-dependent epigenetic alterations of mouse metallothionein-2 gene☆

Hisaka Kurita[a], Seiichiroh Ohsako[a], Shin-ichi Hashimoto[b], Jun Yoshinaga[c], Chiharu Tohyama[a,*]

[a]*Laboratory of Environmental Health Sciences, Center for Disease Biology and Integrative Medicine, Graduate School of Medicine, The University of Tokyo, 7-3-1 Hongo, Bunkyo-ku, Tokyo 113–0033, Japan*

[b]*Department of Molecular Preventive Medicine, Graduate School of Medicine, The University of Tokyo, Hongo, Bunkyo-ku, Tokyo, Japan*

[c]*Department of Environmental Studies, The University of Tokyo, Kashiwanoha, Kashiwa, Chiba, Japan*

Received 14 February 2012; received in revised form 29 April 2012; accepted 7 May 2012

Abstract

Zinc (Zn) deficiency *in utero* has been shown to cause a variety of disease states in children in developing countries, which prompted us to formulate the hypothesis that fetal epigenetic alterations are induced by zinc deficiency *in utero*. Focusing on metallothionein (MT), a protein that contributes to Zn transport and homeostasis, we studied whether and how the prenatal Zn status affects gene expression. Pregnant mice were fed low-Zn (IU-LZ, 5.0 μg Zn/g) or control (IU-CZ, 35 μg Zn/g) diet *ad libitum* from gestation day 8 until delivery, with a regular diet thereafter. Bisulfite genomic sequencing for DNA methylation and chromatin immunoprecipitation assay for histone modifications were performed on the *MT2* promoter region. We found that 5-week-old IU-LZ mice administered cadmium (Cd) (5.0 mg/kg b.w.) have an elevated abundance of *MT2* mRNA compared with IU-CZ mice. Alteration of histone modifications in the *MT2* promoter region having metal responsive elements (MREs) was observed in 1-day-old and 5-week-old IU-LZ mice compared with IU-CZ mice. In addition, prolongation of MTF1 binding to the *MT2* promoter region in 5-week-old IU-LZ mice upon Cd exposure is considered to contribute to the enhanced MT2 induction. In conclusion, we found for the first time that Zn deficiency *in utero* induces fetal epigenetic alterations and that these changes are being stored as an epigenetic memory until adulthood.

Keywords: DNA methylation; Epigenetics; Histone modification; Metallothionein; Zinc

1. Introduction

The malnutritional status *in utero* has been shown to affect the progeny's health and disease states later in life in humans as well as in laboratory animals. Low-birth-weight babies resulted from prenatal malnutrition can be a risk factor for lifestyle-related diseases, such as ischemic heart disease and diabetes [1–4]. This hypothesis has been widely acknowledged and expanded to the concept, named 'Developmental origins of health and disease (DOHaD)' [5]. Recently, rats that were grown under low-protein nutritional conditions *in utero*, or had intrauterine growth retardation have been shown to develop hypertension or type 2 diabetes later in adulthood [6–9]. Moreover, a plethora of published works have shown that extrinsic conditions *in utero*, such as nutrition and environmental chemicals, affect the propensity of the fetus to develop disease states later in adulthood [10–12]. Although the underlying mechanism is still under intensive investigation, there is a widely-acknowledged view that epigenetic alterations, namely, DNA methylation (the covalent addition of a methyl group to the 5′-carbon of cytosine in the CpG dinucleotide) and histone modification (methylation, acetylation, phosphorylation, ADP-ribosylation, and ubiquitination), play a pivotal role in the expression of particular genes, which will subsequently alter the physiological status of the whole organism. Gene expression is suppressed by DNA methylation of the promoter region of a given gene [13], whereas histone modifications regulate chromatin structure and alter gene activity [14]. Such epigenetic alterations could be inherited by succeeding generations [15].

Experimentally, a few studies have shown that zinc (Zn) restriction during pregnancy induces disease states later in life. Rats grown under prenatal or postnatal Zn restriction have been reported to develop hypertension [16] and impairments of learning and memory [17,18] later in adulthood. Pregnant mice fed a Zn-deficient diet *in utero* have shown persistent immunodeficiency for three succeeding generations [19]. Zn is an essential trace element and a key component of approximately 300 enzymes in various types of tissues [20,21]. Zn deficiency induces various disease states in humans, such as immunodeficiency, developmental disorders, alopecia, dysgeusia, skin disorders and anemia. Vegetarians [22], elderly

☆ Grants and Funding Sources: This study was supported by a Grant-in-Aid for Challenging Exploratory Research (21651022) from the Japan Society for Promotion of Science (JSPS) (to CT) and Research Fellowships for Young Scientists (224083) from JSPS and Global COE Program "Medical System Innovation on Multidisciplinary Integration" from MEXT, Japan (to HK).

* Corresponding author. Tel.: +81 3 5841 1431; fax: +81 3 5841 1434.
E-mail address: mtohyama@mail.ecc.u-tokyo.ac.jp (C. Tohyama).

0955-2863/$ - see front matter © 2013 Elsevier Inc. All rights reserved.
http://dx.doi.org/10.1016/j.jnutbio.2012.05.013

persons [23], habitual alcohol drinkers [24], infants and pregnant/parturient women [22] have the tendency to develop Zn deficiency. In addition, maternal Zn deficiency during pregnancy induces pregnancy complications, delayed delivery, and low-body-weight birth [25]. Zn deficiency is responsible for 4.4% of deaths of children aged 6–59 months in developing countries [26].

Metallothionein (MT), a low-molecular weight protein, has been shown to be involved in the transport, metabolism and homeostasis of heavy metal ions, such as Zn and copper, in tissues and cells. One-third of their amino acid residues of this protein are cysteine residues without a disulfide bond. This characteristic enables MTs to play a role in the transport and inactivation/detoxification of metals [27,28]. Aside from the metabolism and homeostasis of heavy metals, MT has been known to protect cells from oxidative stress and inflammation elicited by various environmental stimuli including heavy metals. Among the four MT isoforms known so far, MT1 and MT2 exist in nearly all types of cells in the body. It has been established that the expression of *MT1/2* genes is induced by metal ions, such as Cd, Zn, Cu and Hg [27]. For the up-regulation of *MT1/2* transcription upon exposure to these metal ions, metal responsive elements (MREs) located in the promoter region are essential. A limited line of experimental evidence showed that metal transcription factor 1 (MTF1) [29] will bind to the MRE motif upon exposure to at least Zn ions, and the Zn-ion-bound MTF1 forms a complex with p300 and Sp1, and then this complex is recruited to MREs of the *MT1* promoter region [30].

The effects of prenatal zinc deficiency on MT regulation have been studied. Pregnant mice were fed either a control diet (100 μg Zn/g) or a low-Zn diet (5.0 μg Zn/g) from gestation day 7 to delivery, and both groups of dams were given the control diet after delivery. Although the Zn and MT levels in pups born to these two groups of dams were similar at postnatal day 3, serum IgM concentrations were significantly lower in adulthood in the mouse offspring born to dams given the low-Zn diet than in the offspring born to control dams. Moreover, when the mouse offspring was given Zn injections to stimulate MT synthesis, the mice deprived of Zn while *in utero* had markedly higher MT levels in the liver than control mice later in adulthood [31].

Collectively, prenatal Zn deficiency has been shown to induce disease states, which is presumably due to epigenetic alterations. However, nearly no studies to elucidate the molecular basis of disease states induced by prenatal Zn deficiency are available. Thus, we have hypothesized that fetal epigenetic alterations can be induced by Zn deficiency *in utero* and alter the physiological conditions that will lead to the onset of disease conditions later in adulthood. In this study, we developed an experimental animal model of prenatal Zn deficiency and studied whether Zn deficiency *in utero* exerts fetal epigenetic alterations in *MT1/2* genes.

2. Materials and methods

2.1. Reagents

The following reagents were purchased from the manufacturers described in parentheses: RNase A, mouse monoclonal anti-β-actin IgG1 and CellLyticNuCLEAREx-traction kit (Sigma-Aldrich, St Louis, MO, USA); RNeasy Mini kit, QIAquick PCR Purification kit, QIAquick Gel Extraction kit and QIAprep Spin Miniprep kit (Qiagen K.K., Tokyo, Japan); Lipofectamine 2000 (Invitrogen, Carlsbad, CA, USA); Wizard DNA Clean-Up system, pGEM-T Easy Vector, pGL4.0 Luciferase Reporter Vector, phRL-TK Vector and Dual-Luciferase Reporter Assay System (Promega, Madison, WI, USA); proteinA agarose/salmon sperm DNA, rabbit polyclonal anti-acetylated histone H3 IgG, rabbit polyclonal anti-acetylated histone H4 IgG, rabbit polyclonal anti-acetylated histone H3 lysine14 IgG and Immobilon-P transfer membrane (MilliPore, Billerica, MA, USA); proteinase K, Blocking One and Chemi-Lumi One (Nacalai Tesque, Kyoto, Japan, USA). *Bam* HI, *Aci* I, *Kpn* I, *Xho* I and *Dpn* I were purchased from New England Biolabs Japan (Tokyo, Japan); rabbit polyclonal anti-MTF1 IgG and goat polyclonal anti-lamin B (Santa Cruz Biotechnology, Santa Cruz, CA, USA); Big Dye Terminator v3.1 Cycle Sequencing kit (Applied Biosystems, Foster City, CA, USA); Immunopure goat anti-rabbit IgG, F(ab′)2, peroxidase conjugated, ImmunoPure goat anti-mouse IgG, F(ab′)2, peroxidase conjugated and Immuno Pure rabbit anti-goat IgG, F(ab′)2, peroxidase conjugated (Thermo Fisher Scientific, Rockford, IL, USA); rabbit polyclonal anti-acetylated histone H3 lysine9 IgG and rabbit polyclonal anti-trimethylated histone H3 lysine4 IgG (Cell Signaling Technology, Danvers, MA, USA). LightCycler480 SYBR Green I Master (Roche Diagnostics Japan, Tokyo, Japan); Minisart SRP 15 (Sartorius Stedim Biotech, Goettingen, Germany). IGEPAL-CA630 (Wako Pure Chemical, Osaka, Japan); PrimeScript RT reagent kit, SYBR Premix Ex Taq, TaKaRa Ex Taq, LA Taq and T4 polynucleotide kinase (TaKaRa BIO, Otsu, Japan). *Not* I, DH5α and KOD -Plus (Toyobo, Osaka, Japan); Ligation Convenience kit and ISOGEN (Nippon Gene, Tokyo, Japan); all other reagents of analytical grade (Sigma-Aldrich, Invitrogen and Wako Pure Chemical); all oligonucleotides (Hokkaido System Science, Sapporo, Japan).

2.2. Animals

C57BL/6J strain pregnant ($n=44$) and male mice ($n=18$) were purchased from CLEA Japan. The mice were housed in a room with temperature at 23±1°C and humidity at 50±10% on a 12/12-h light–dark cycle. We used three kinds of rodent chow. Laboratory rodent chow (50 μg Zn/g; Labo MR Stock, Nosan) was given to mice unless specifically described. Low-Zn diet (5.0 μg Zn/g) or control diet (35 μg Zn/g) (CLEA Japan) was used in Zn-deficiency experiments. According to the previous studies [32,33], zinc concentration in diet (35 μg Zn/g) was found to be high enough to be used for a control diet group. These chows and deionized water were provided *ad libitum*. For this study, male mice were used unless specifically described. The experiments protocols using mice were approved by the Animal Care and Use Committee of the Graduate School of Medicine, the University of Tokyo.

2.3. Experiments on Zn deficiency in utero

Pregnant mice were fed a Labo MR Stock rodent chow until gestation day 7, and the chow was replaced with a low-Zn diet or a control diet thereafter until delivery. On the day of birth, two to three male pups per dam were randomly adopted from fourteen dams to minimize possible litter effects and to make two groups: (1) *in utero* low-Zn (IU-LZ) mice and (2) *in utero* control (IU-CZ) mice. The pups were decapitated by scissors, and their livers were harvested. All the liver tissues except those used for chromatin immunoprecipitation (ChIP) assay were immediately frozen in liquid nitrogen, and kept at −80°C until analyses. Livers used for the ChIP assay were immediately minced by scissors and subjected to the subsequent processes as described in the ChIP assay section below. The number of pups for each dam was adjusted to be 6 to 7 pups by adoption from other dams on the day of birth. The dams were given Labo MR Stock rodent chow from the delivery to weaning. After weaning, male pups were given Labo MR Stock rodent chow thereafter.

When IU-CZ mice and IU-LZ mice became 5 weeks old, they were administered orally with a single dose of cadmium (Cd) (5.0 mg kg^{-1} b.w.). Mice were sacrificed by cervical dislocation, and livers were harvested 0, 1 and 6 h post Cd administration (Fig. 1A).

2.4. Experiment on Zn deficiency in adulthood

Male mice aged 10 weeks were fed a low-Zn(AD-LZ) diet or a control (AD-CZ) diet *ad libitum* for 12 days, and then sacrificed by cervical dislocation to harvest the liver. Other mice were fed Labo MR Stock rodent chow for another 30 days, and administered orally a single dose of Cd (5.0 mg kg^{-1} b.w.). Livers were collected 6 h after Cd administration (Fig. 1B).

2.5. Measurement of Zn and Cd concentrations

Livers (approx. 0.1 g) and blood (approx. 0.2 g) specimens were digested in 2 ml of concentrated nitric acid in glass test tubes. The temperatures were kept at 80°C for 1 h, with a gradual increase with 10°C for 1 h each to 130°C. When the acid-digested specimens were became transparent, they were diluted with 1% $HNO_3$and filtered with Minisart SRP 15 and determined for Zn and Cd concentrations by inductively coupled plasma mass spectrometer (Agilent 7500ce; Agilent Technologies).

2.6. RNA isolation and reverse transcription

Total RNA was isolated using RNeasy Mini Kit and then reverse-transcribed using PrimeScript RT reagent Kit, according to the manufacturer's instructions.

2.7. DNA isolation

DNA was isolated using ISOGEN, according to the manufacturer's instructions and purified by phenol/chloroform extraction method.

2.8. Quantitative polymerase chain reaction

Quantitative polymerase chain reaction (qPCR) analysis was performed using SYBR Premix Ex Taq and amplified by LightCycler under the following conditions: 95°C/10 s ×1 cycle; 95°C/5 s, 60°C/30 s, ×45 cycles or using LightCycler480 SYBR Green I Master and amplified by LightCycler480 under the following conditions: 95°C/5 min ×1 cycle; 95°C/15 s, 60°C/10 s, 72°C/30 s ×45 cycles. Primers used in the qPCR analysis

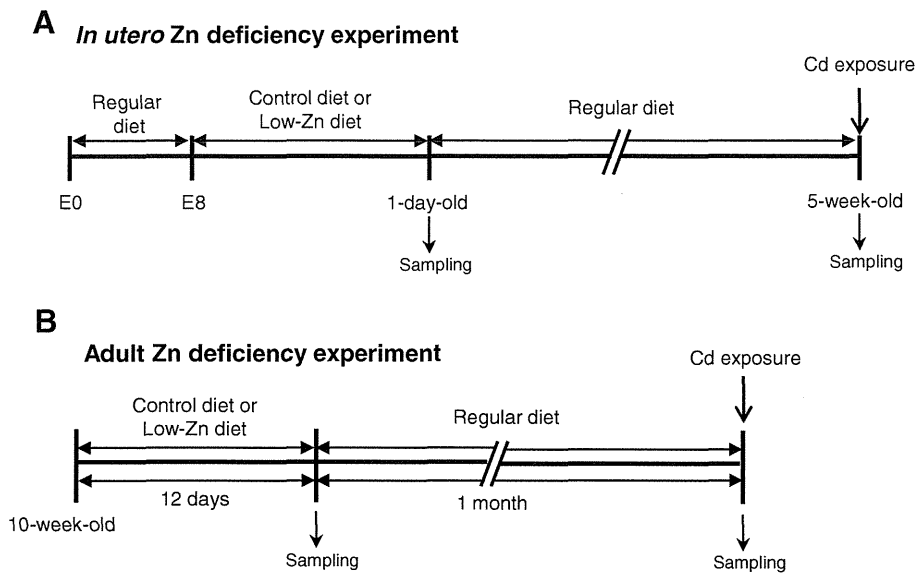

Fig. 1. Study design. (A) Pregnant mice were fed a regular diet until Gestation Day 7, and the chow was replaced with a low-Zn diet or control diet thereafter until delivery. On the day of birth, male pups were divided into two groups: (1) *in utero* low-Zn (IU-LZ) mice and (2) *in utero* control-Zn (IU-CZ) mice. Livers were harvested from a group of 1-day-old male pups. The dams were given Labo MR Stock rodent chow from the delivery to weaning. After weaning, male pups were given Labo MR Stock rodent chow thereafter. When IU-CZ mice and IU-LZ mice became 5 weeks old, they were administered orally a single dose of Cd (5.0 mg kg^{-1} b.w.) and sacrificed by cervical dislocation, and livers were collected 0, 1 and 6 h after Cd administration. (B) Male mice aged 10 weeks were fed a low-Zn diet (AD-LZ) or control diet (AD-CZ) ad libitum for 12 days and then sacrificed by cervical dislocation, and livers were collected. Other mice were fed a regular diet for another 30 days and administered orally a single dose of Cd (5.0 mg kg^{-1} b.w.). Livers were collected 6 h after Cd administration.

are described in Table S1. All primer sets were designed by using Primer3 [34]. All quantitative data were calculated by dividing the copy number of targets by the original RNA concentration, according to a previous study [35].

2.9. Bisulfite genomic sequencing

Mouse genomic DNA was digested with *Not* I and bisulfite conversion reaction was performed as previously described [36]. The bisulfite-treated DNA was cleaned up using Wizard DNA Clean-Up system and amplified by nested PCR method using Ex Taq under the following conditions for the first and second PCRs: 94°C/2 min ×1 cycle; 94°C/2 min, 50°C/2 min, 72°C/3 min, ×5 cycles; 94°C/2 min, 50°C/2 min, 72°C/30 s, ×5 cycles; 72°C/5 min ×25 cycles. Each primer set for the nested amplification is shown in Table S2. All primers were designed using Methyl Primer Express Software v1.0 (Applied Biosystems). The amplified DNA was purified using QIA quick PCR Purification kit and ligated into pGEM-T Easy Vector and transformed into DH5α. Colony PCR was performed to amplify target DNAs using Ex Taq and M13 primers. The PCR products were sequenced using Big Dye Terminator v3.1 Cycle Sequencing kit and analyzed using 3730 DNA Analyzer (Applied Biosystems).

2.10. Methylation frequency analysis

Purified DNA was digested with *Bam* HI. The digested DNA solution was divided into two portions. One portion was digested with the methylation-sensitive *Aci* I, whereas the other was kept as it was. These *Aci* I-digested and non-digested DNA was subjected to qPCR using SYBR Premix Ex Taq and amplified by LightCycler under the following conditions: 95°C/10 s ×1 cycle; 95°C/5 s, 60°C/15 s, 72°C/20 s, ×40 cycles. Ch-R1 primer sets described in Table S3. The DNA methylation frequency was represented as copy numbers of *Aci* I-digested DNA/copy numbers of non-digested DNA.

2.11. Chromatin Immunoprecipitation assay

The ChIP assay was performed by the essentially same method as previously described [37], with some modifications: the minced mouse liver was cross-linked with 1% formaldehyde for 10 min at room temperature, followed by addition of glycine to be a final concentration of 125 mM and by incubation for 5 min. The cross-linked liver specimen was homogenized using a Dounce homogenizer (catalog# 432–1273, Wheaton) and washed with phosphate-buffered saline three times. The pellet was dissolved in lysis buffer (5.0 mM Tris–HCl, pH 8.1, containing 1.0% sodium docecyl sulfate [SDS], 10 mM EDTA). It was subjected to sonication by Bioruptor UCD-250HSA (Cosmo Bio) to make an average chromatin fragment size to be 200 to 1000 bp. ProteinA agarose and salmon sperm DNA were added to the fragmented DNA solution, and it was incubated for 1 h at 4°C to eliminate nonspecific substances. An aliquot of the sample was diluted by adding dilution buffer (16.6 mM Tris–HCl, pH 8.1, containing 0.01% SDS, 1.1% Triton X-100, 1.2 mM EDTA, and 167 mM NaCl) and incubated with an antibody at 4°C overnight. The sample was immunoprecipitated with ProteinA agarose and salmon sperm DNA and washed consecutively with the following four kinds of buffers: low-salt immune complex buffer (20 mM Tris–HCl, pH 8.1, containing 0.1% SDS, 1.0% Triton X-100, 2.0 mM EDTA, and 0.15 M NaCl), high-salt immune complex buffer (20 mM Tris–HCl, pH 8.1, containing 0.1% SDS, 1.0% Triton X-100, 2.0 mM EDTA, and 0.5 M NaCl), LiCl immune complex buffer (10 mM Tris–HCl, pH 8.1, containing 1.0% IGEPAL-CA630, 1.0 mM EDTA, 0.25 M LiCl, 1.0% deoxycholic acid), and TE buffer. The immunoprecipitated DNA was eluted with buffer (0.1 M $NaHCO_3$, pH 8.5, containing 1.0% SDS and 10 mM DTT). Cross-link was removed by an addition of 5.0 M NaCl with incubation at 65°C overnight. The resultant DNA was treated with RNase A for 30 min and proteinase K for 1 h, and the DNA was purified by using QIA quick PCR Purification kit. Quantitative real time PCR was carried out with the DNA using SYBR Premix Ex Taq and amplified by LightCycler under the following conditions: 95°C/10 s ×1 cycle; 95°C/5 s, 60°C/15 s, 72°C/20 s, ×60 cycles or using LightCycler480 SYBR Green I Master and amplified by LightCycler480 under the following conditions: 95°C/5 min ×1 cycle; 95°C/15 s, 60°C/10 s, 72°C/30 s ×65 cycles. Primers used in this assay are described in Table S3.

2.12. Western blotting

Nuclear and cytosolic proteins were extaracted from mouse liver using CellLyticNuCLEARExtraction kit according to the manufacturer's instructions. The protein specimens (25 μg protein/lane) were separated on a 10% SDS-polyacrylamide gel and blotted on an Immobilon-P transfer membrane. The blotted membrane was blocked with Blocking One at room temperature for 1 h. Primary antibody was applied at 4°C overnight, with a dilution factor as described in parentheses: anti-MTF IgG (1:10,000), β-actin IgG1 (1:4,000) and anti-laminB IgG (1:1,000). The 5,000-fold diluted the secondary antibody was applied at room temperature for 1 h. The antigen-antibody complexes were visualized by using Chemi-Lumi One. For quantitative analysis, the chemiluminescence intensity of respective bands was quantified using CS analyzer ver.2.02b (ATTO).

2.13. Plasmid constructs

The DNA fragment containing *Kpn* I and *Xho* I restriction sites of −2,166 to −17 in the *MT2* promoter was amplified from mouse hepatic DNA by PCR method using LA Taq under the following conditions: 95°C/1 min ×1 cycle; 95°C/30 s, 60°C/1 min, 72°C/2 min, ×30 cycles; 72°C/10 min ×1 cycle. Primers used for the qPCR are described in Table S4. This fragment was inserted into pGEM-T Easy Vector using Ligation Convenience kit. This plasmid was transformed to DH5αand cloned. The cloned plasmid was digested by *Kpn* I and *Xho* I. The inserted fragment was separated by electrophoresis in agarose gel and purified by QIAquickGel extraction kit. This purified fragment was inserted into pGL4.0 Luciferase Reporter Vector digested by *Kpn* I and *Xho* I. This construct was named as *pGL4MT2 -2166*. The *MT2* MRE-deletion constructs

(Fig. 4B) were made from *pGL4MT2 -2166* as a template by inverse PCR method as follows. The MRE-deletion fragments were amplified from *pGL4MT2-2166* construct by PCR method using KOD-Plus under the following conditions: 94°C/2 min ×1 cycle; 98°C/10 s, 68°C/2 min, ×10 cycles. Primers used are described in Table S4. The remaining pGL4MT2 construct was digested by *Dpn* I. The 5′-prime of MRE-deletion fragments was phosphorylated by T4 polynucleotide kinase. These fragments were self-ligated by Ligation Convenience kit and transformed to DH5α. The cloned MRE-deletion constructs were purified by QIAprep Spin Miniprep kit.

2.14. Transfection and luciferase reporter assay

Hepa1c1c7 cells purchased from American Type Culture Collection were maintained in DMEM, supplemented with 10% FBS, 100 U/ml penicillin, 0.01% streptomycin, 0.01% sodium pyruvate, 0.03% L-glutamine, and 55 μM 2-mercaptethanol at 37°C under 5.0% CO_2 condition. In the first experiment, to examine induction of *MT2* mRNA by Cd exposure, cells were seeded at a density of 4.4×10^5 cells per well in a six-well multiplate. After 24 h, cells were exposed to 5.0 μM Cd for a specified time and harvested for qPCR analysis. In the second experiment, to study transcription activity of *MT2*, cells were seeded and incubated at a density of 4.4×10^5 cells per well in a 48-well multiplate for 24 h, followed by co-transfection with phRL-TK Vector and each MT2 reporter construct using Lipofetamine2000 for another 24 h. Then, the cells were exposed to 5.0 or 10.0 μM Cd for 24 h, and reporter assays were conducted using the Dual-Luciferase Reporter Assay System, following the manufacturer's instructions.

2.15. Statistical analysis

All results are expressed as mean±standard errors. Statistical analysis was performed using IBM SPSS Statistics ver. 19.0 (IBM). A two-way analysis of variance (ANOVA), followed by Bonferroni's post hoc test was performed to compare means of mRNA expression, histone modification, and protein expression among IU-LZ and IU-CZ or AD-LZ and AD-CZ groups of 5-week-old mice as well as reporter gene assay data. Student's *t* test was used for other analyses to compare between IU-LZ and IU-CZ groups or AD-LZ and AD-CZ groups. A *P*-value of less than .05 was considered to be statistically significant.

3. Results

3.1. Zn and Cd concentrations in liver

Pregnant mice fed the low-Zn diet had a significantly lower blood Zn concentration than those fed the control diet (3.98±0.04 μg/g, $n=3$ vs. 4.92±0.10 μg/g, $n=6$). As for the mouse progeny, no significant difference in body weight was observed between IU-LZ and IU-CZ mice on postnatal days 1, 27, and 35 (data not shown). The hepatic Zn concentration was significantly lower in 1-day-old IU-LZ mice than in IU-CZ mice (20.4±1.8 μg/g tissue, $n=13$ vs. 37.3±2.9 μg/g tissue, $n=18$), but they became similar by postnatal week 5 (Table 1). No significant changes in hepatic Zn and Cd concentrations were observed between IU-LZ and IU-CZ mice 6 h after Cd administration (Table 1).

3.2. Induction of MT1 and MT2 mRNAs upon Cd exposure in the liver of mice fed a Zn deficient-diet

The abundances of *MT1* and *MT2* mRNAs in the liver were examined in 5-week-old mice with and without Cd exposure. The abundances of *MT1* mRNAs in IU-LZ and IU-CZ mice at 6 h after Cd administration were significantly higher than those in the corresponding groups of mice at 0 h (Fig. 2A). Similar results to *MT1* mRNA were observed for *MT2* mRNA although no statistically significant observations were obtained for the abundance of *MT2* mRNA in IU-CZ before and after Cd administration (Fig. 2B). Without Cd exposure, the abundances of *MT1* and *MT2* mRNAs of IU-LZ mice and those of IU-CZ mice were not different from each other (Fig. 2A, B). Six hours after Cd administration, the abundances of *MT1* mRNA was similar between IU-LZ and IU-CZ mice (Fig. 2A), whereas the abundances of *MT2* mRNA was higher in IU-LZ mice than in IU-CZ mice (Fig. 2B). Although the elevated expression of *MT* genes has been shown to be mediated by MTF1 upon Zn administration [30], no significant alterations in *MTF1* mRNA abundance were found between IU-LZ and IU-CZ mice after Cd administration (Fig. 2C).

Table 1
Zn and Cd concentrations in the liver of 5-week-old mice born to dams given a low-Zn diet or a control diet and those before or after Cd administration

Experimental group	Zn (μg/g tissue)		Cd (μg/g tissue)	
	Unexposed	Cd-exposed	Unexposed	Cd-exposed
IU-CZ	32.2±0.5 (5)	42.8±1.2 (6)	n. d. (5)	0.71±0.13 (6)
IU-LZ	32.6±0.5 (9)	42.1±0.8 (11)	n. d. (9)	0.89±0.11 (11)

Data are expressed as mean±S.E.M. with a number of animals in parentheses.
n.d., not detectable.

3.3. Methyl-CpG status of MT2 gene altered by prenatal Zn deficiency

We hypothesized that the *MT2* mRNA abundance in IU-LZ mice is enhanced by epigenetic alterations. Then, we analyzed the DNA methylation frequency by bisulfite sequencing with a special reference to the methyl-CpG status in the *MT2* promoter region and

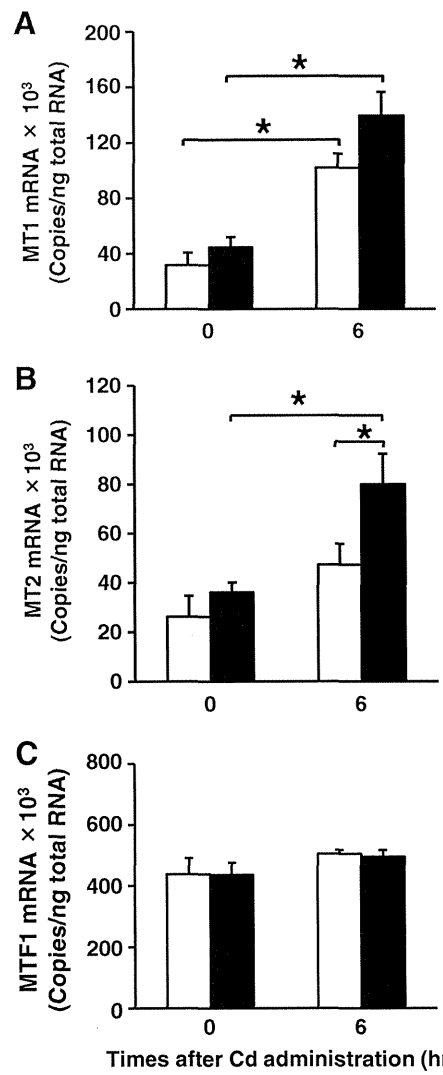

Fig. 2. Abundances of *MT1*, *MT2* and *MTF1* mRNA upon Cd exposure in liver of 5-week-old pups fed a low-Zn diet: (A) *MT1* mRNA, (B) *MT2* mRNA and (C) *MTF1* mRNA. IU-CZ (open) and IU-LZ (closed) groups. Data are expressed as mean±SEM (IU-CZ 0 h, $n=5$; IU-LZ 0 h, $n=9$; IU-CZ 6 h, $n=6$; IU-LZ 6 h, $n=11$). Statistically significant difference was determined by two-way ANOVA, followed by *post hoc* Bonferroni's test (*$P<.05$).

compared the DNA methylation frequency between IU-CZ and IU-LZ mice in 5-week-old mice. The locations of the transcription start site, MREs, TATA box, and target regions amplified by primer sets are shown in Fig. 3A. The CpG islands, from the −480 to +140 bp region (BS-R4 and BS-R5) of the *MT2* gene, which include MREs, were not methylated in IU-CZ and IU-LZ mice. Although the vast majority of CpG sites in the promoter region showed absolutely no methylation in either animal groups, the −834 and −820 bp CpG sites in IU-LZ mice were more frequently methylated than those in IU-CZ mice. Since the −820 bp CpG site (Fig. 3B; arrow) has the CCGC sequence that can be recognized by the methyl-sensitive restriction enzyme *Aci* I, methylation frequency analysis using *Aci* I was performed at the −820 CpG

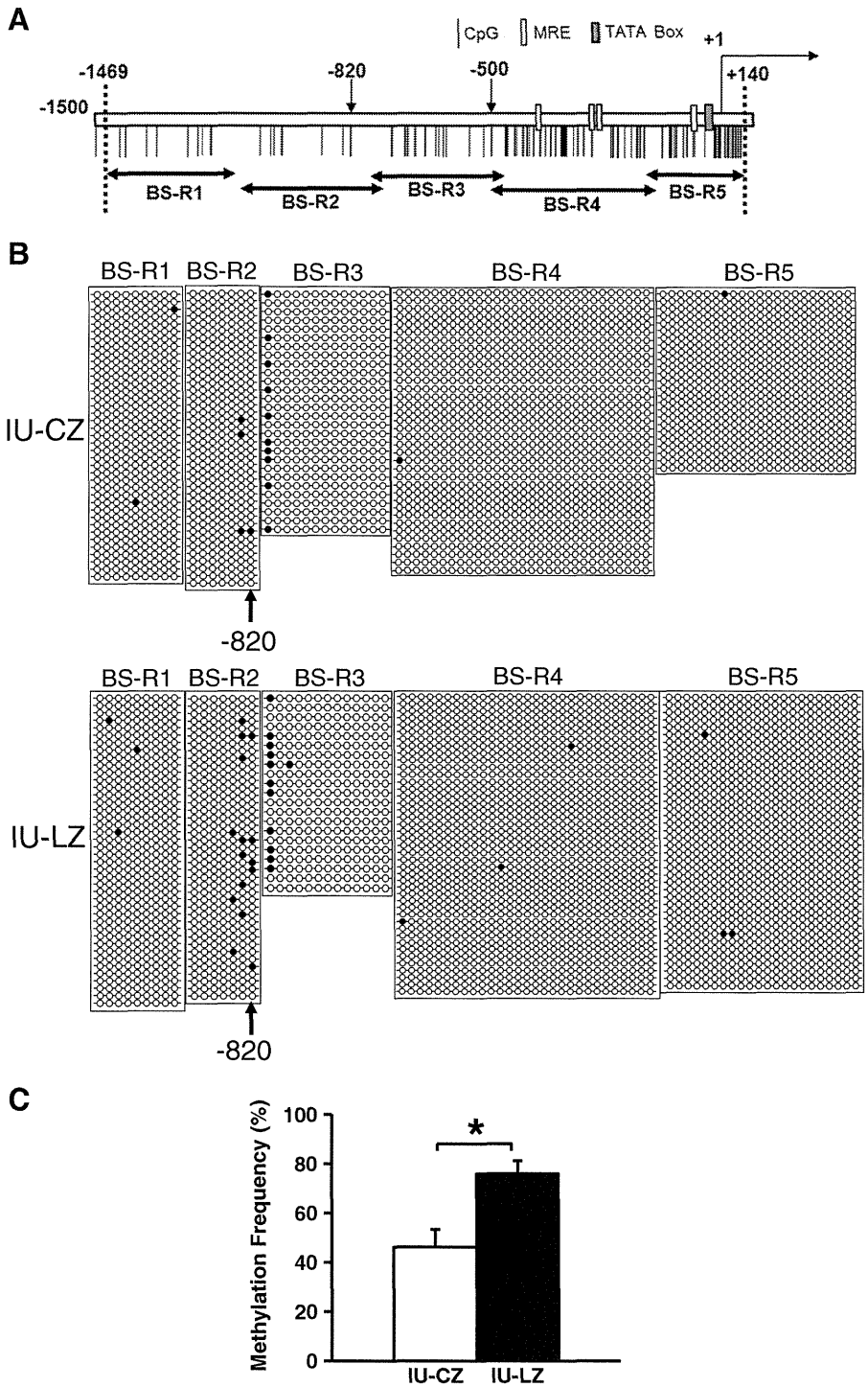

Fig. 3. Comparison of DNA methylation status and frequency of 5′-flanking region of *MT2* gene in livers of 5-week-old mice grown under perinatal Zn deficiency. (A) Target regions of *MT2* gene analyzed by bisulfite genomic sequencing. The locations of transcription start site, MREs and TATA box are shown in a previous study [50]. (B) DNA methylation status and frequency of 5′-flanking region of *MT2* of the control (IU-CZ: opened) and Zn deficiency (IU-LZ: closed) mice: CpG dinucleotides are represented by circles (●, methylated cytosine; ○, unmethylated cytosine). (C) Methylation frequency of -820 bp CpG determined by quantitative PCR with methylation-sensitive restriction enzyme. Open (IU-CZ mice) and closed (IU-LZ mice) columns are presented. Data are expressed as mean±S.E.M. (IU-CZ, $n=5$; IU-LZ, $n=9$). Statistically significant difference was determined by Student's t test (*$P<.05$).

site in the IU-CZ (n=6) and IU-LZ (n=9) mouse samples. A significant increase in DNA methylation frequency was observed at the −820 CpG site in IU-LZ mouse samples, suggesting the association of prenatal Zn deficiency with a high methylation status (Fig. 3C), which is consistent with the result of bisulfite sequencing (Fig. 3B).

3.4. MT2 promoter analysis

No data on *MT2* promoter functional analysis in various animal species is available. Thus, using an *MT2* gene-promoter-driven luciferase reporter gene assay, we confirmed that *MT2* mRNA abundances were significantly induced in Hepa1c1c7 cells as early as 3 h after Cd addition to the medium (Fig. 4A). For deletion analysis, we made six deletion constructs from an original construct connected with a 2,166 bp flanking region to the pGL4 vector (*pGL4MT2-2166*), on the basis of the strategy that the possible functionalities of the four MREs can be evaluated (Fig. 4B). Hepa1c1c7 cells that were transfected with either of the *pGL4MT2-2166, pGL4MT2-397, pGLMT2-307* or *pGLMT2-287*construct were found to have significantly elevated transcription activity upon exposure to 5.0 or 10.0 μM Cd (Fig. 4B). However, almost no additional induction above a constitutive level was observed by Cd treatment in the following three transfected cell lines: cells transfected with *pGL4MT2Δ-397-37* construct from which all four MRE motifs were deleted, those transfected with *pGL4MT2-65* having an MRE motif and those transfected with *pGL4MT2-37* having no MRE motif (Fig. 4B). Collectively, only one MRE located between a −287 to −65 bp region are suggested to play a crucial role in the induction of *MT2* mRNA by Cd in these cells.

3.5. Histone modifications of MT2 gene altered by prenatal Zn deficiency

We applied the ChIP assay to the four target regions (Ch-R1, Ch-R2, Ch-R3 and Ch-R4) of the *MT2* promoter regions, in 5-week-old mice, which contain MREs or −820 CpG, to examine whether histone modifications are altered by the Zn status in the prenatal period (Fig. 5A). We found that the basal amounts of AcH3 at Ch-R1 and Ch-R3, AcH4 at Ch-R1 and Ch-R2 and AcH3K14 at Ch-R3 in IU-LZ mice are significantly higher than those in IU-CZ mice (Fig. 5B, C and E). In Cd-exposed mice, histone modification levels in IU-LZ mice in comparison with those in IU-CZ mice were significantly increased: AcH3 (Fig. 5B) and AcH4 (Fig. 5C) levels in Ch-R2, Ch-R3, and Ch-R4; AcH3K9 (Fig. 5D) levels at Ch-R2 and Ch-R3; AcH3K14 levels in Ch-R1, Ch-R2, Ch-R3 and Ch-R4 (Fig. 5E); and H3K4me3 levels at Ch-R3 (Fig. 5F).

In IU-LZ mice, Cd administration significantly increased the AcH3K14 levels at Ch-R1 and Ch-R2 (Fig. 5E) and H3K4me3 levels at Ch-R3 (Fig. 5F), whereas it significantly decreased the AcH3 (Fig. 5B) and AcH4 (Fig. 5C) levels at Ch-R1. It is not known why Cd exposure reduced histone acetylation in the Ch-R1 region. However, this region is not considered to be responsible for transcription. Next, to determine whether these histone modifications occurred in the newborn livers, we analyzed *MT2* promoter regions in the liver from the 1-day-old pups born to dams given a Zn deficient diet during gestation. The abundances of *MT1, MT2* and *MTF1* mRNAs in IU-LZ

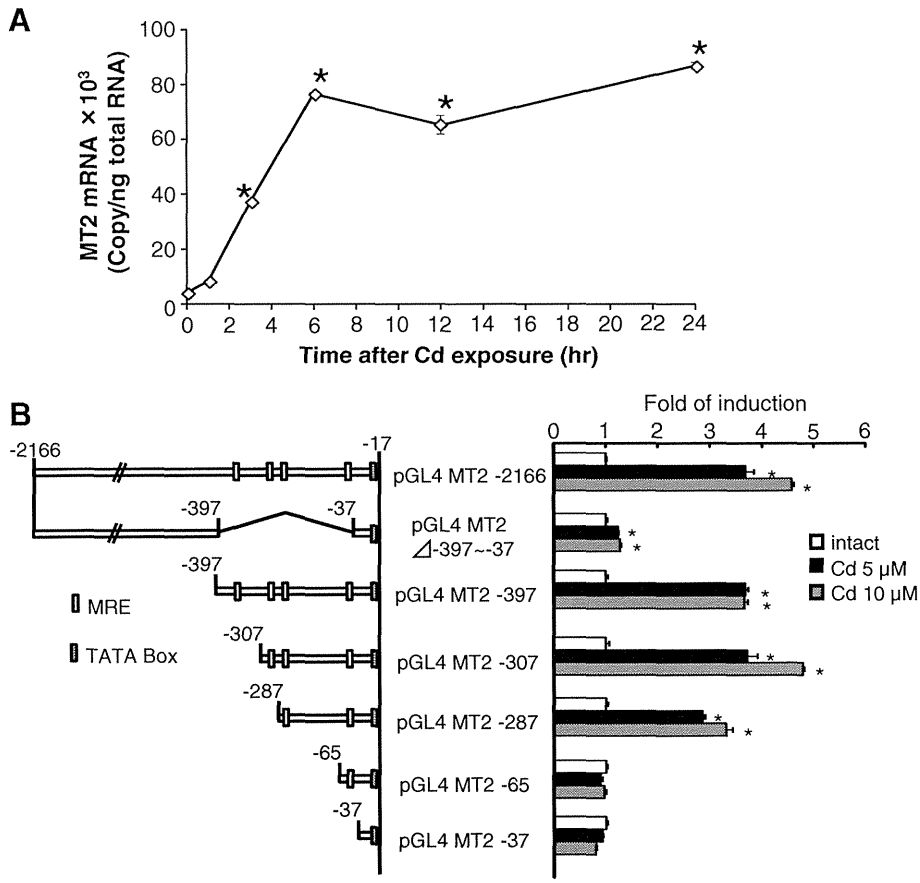

Fig. 4. *MT2* promoter analysis using reporter gene assay. (A) Abundance of *MT2* mRNA in Hepa1c1c7 cells at 0, 3, 6, 12 and 24 h after 5.0 μM Cd treatment. Data are expressed as mean±S.E.M. (*n*=3 per group). Statistically significant difference was determined by one-way ANOVA, followed by post hoc Bonferroni's test (*P<.05 vs. 0 h). (B) Structure of MT2 MRE-deletion constructs (left). Reporter gene activity in Hepa1c1c7 cells transfected with MT2 MRE-deletion constructs at 24 h after 5.0 and 10.0 μM Cd treatment (right). Data are expressed as mean±S.E.M. (*n*=3 per group). Statistically significant difference was determined by one-way ANOVA, followed by post hoc Bonferroni's test at each construct (*P<.05 vs. intact).

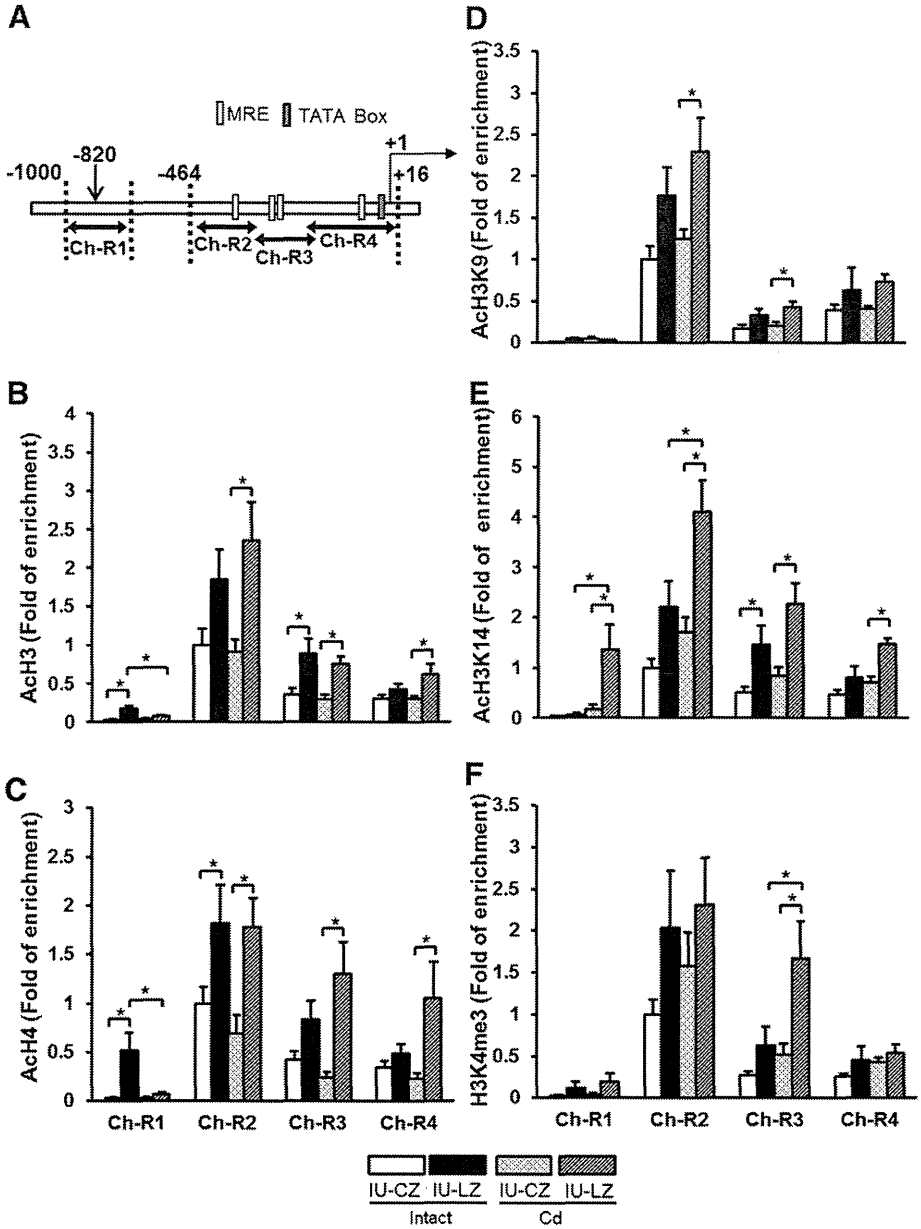

Fig. 5. Changes in histone modification levels in *MT2* promoter regions in 5-week-old mice grown under prenatal Zn deficiency. The livers were collected before and 6 h after Cd administration. (A) Target regions of *MT2* promoter for ChIP assay and localizations of transcription start site, MREs and TATA box are shown in a the previous study [50]. Changes in levels of (B) acetylated histone H3, (C) acetylated histone H4, (D) acetylated histone H3 lysine 9, (E) acetylated histone H3 lysine 14, and (F) tri-methylated histone H3 lysine 4. Open (IU-CZ intact mice), closed (IU-LZ intact mice), dotted (IU-CZ Cd-exposed mice), and diagonal (IU-LZ Cd-exposed mice) columns are presented. Data are expressed as mean±S.E.M. (n=8 per group). Statistically significant difference was determined by two-way ANOVA, followed by post hoc Bonferroni's test at each region (*P<.05).

mice was not altered in comparison with those in IU-CZ mice (Fig. 6A).The AcH3 levels at Ch-R2 and Ch-R3 were significantly higher in IU-LZ mice than in IU-CZ mice (Fig. 6B). The AcH4 levels at Ch-R2 in IU-LZ mice tended to increase in comparison with those in IU-CZ mice (Fig. 6C). These results suggest that the histone acetylation level was already initiated to increase during the perinatal stage by the Zn deficiency *in utero*.

3.6. Zn deficiency in utero prolonged MTF1 binding to the MT2 promoter region upon Cd administration

Since the epigenetic alterations as shown in the previous section suggested the loosening of the chromatin structure in the *MT2* promoter region, we investigated whether Cd exposure *in vivo* affects the status of MTF1binding to a particular region (Ch-R1, Ch-R2, Ch-R3, and Ch-R4) in the *MT2* promoter by the ChIP assay (Table 2). The amounts of MTF1 bound to Ch-R2, Ch-R3 and Ch-R4 were greater at 1 h than those at 0 and 6 h after Cd administration in all the animals (Table 2). The amount of MTF1 bound to Ch-R1, which does not have an MRE motif, was not detected at these time points (data not shown).

The amounts of MTF1bound to Ch-R3 and Ch-R4, but not Ch-R2 were observed to be significantly higher in IU-LZ mice than in IU-CZ mice 6 h after Cd administration, whereas no difference in the amounts of MTF1 bound to these regions was found between the IU-CZ and IU-LZ mice 1 h after Cd administration, which suggests the prolongation of MTF1 binding to the MRE motif (Table 2). The amounts of MTF1 protein in both nucleus and cytosol were unchanged between the IU-LZ and IU-CZ mice and between before

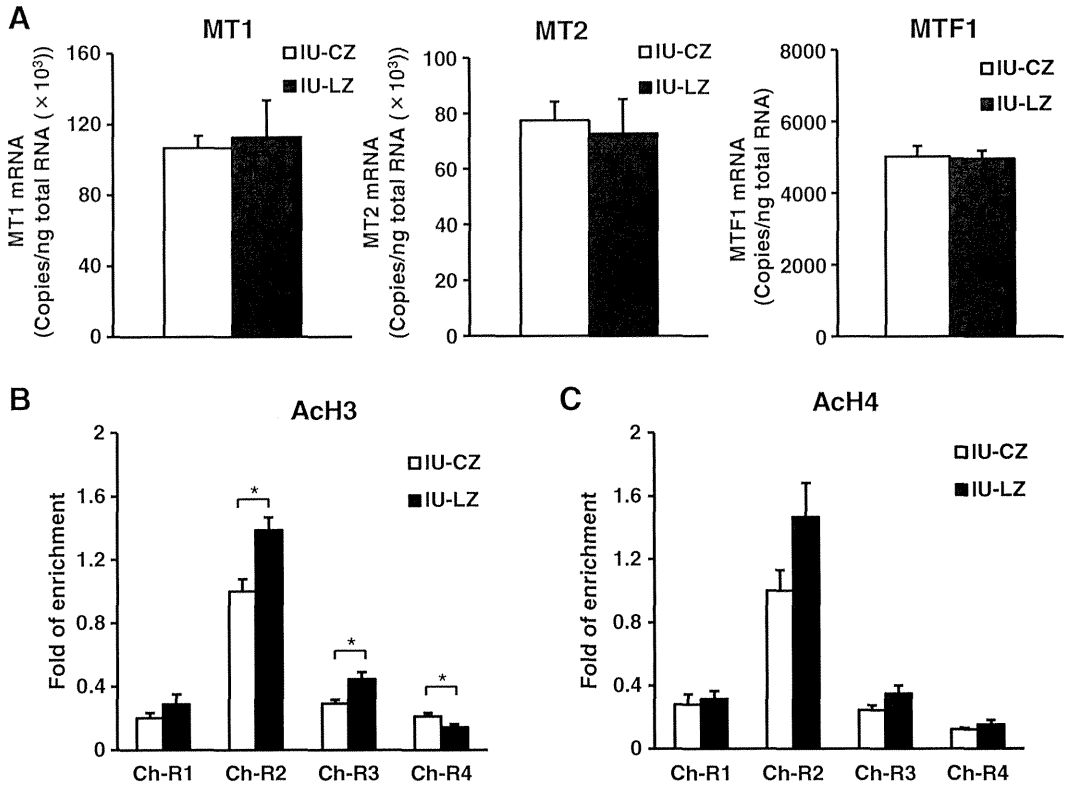

Fig. 6. (A) Abundances of *MT1*, *MT2* and *MTF1* mRNAs and (B) levels of acetylated histone H3 and (C) histone H4 in the *MT2* gene in the liver in 1-day-old male pups grown under Zn deficiency condition. The target regions for histone modifications analysis are shown in Fig. 5A. Data are expressed as mean±S.E.M. ($n=6$ per group). Statistically significant difference was determined by Student's t test at each region (*$P<.05$).

and 6 h after Cd administration (Fig. 7), suggesting that the total amounts of MTF1 protein in the liver were not altered by prenatal Zn deficiency or Cd administration.

3.7. Epigenetic alterations induced by Zn-deficiency in adulthood

To determine whether the epigenetic alterations induced by Zn deficiency are a temporally specific event, adult mice were fed a low-Zn diet or a control diet for 12 days, and the liver was collected just after the end of this period and subjected to the epigenetic analyses. In the AD-CZ and AD-LZ mice, no significant differences in the mRNA abundances of *MT1*, *MT2* and *MTF1* were found (Fig. 8A).Although the levels of AcH3 (Fig. 8B) and AcH3K14 (Fig. 8E) at Ch-R1 in the *MT2* promoter of AD-LZ mice were significantly higher than those of AD-CZ mice, the differences were not conspicuous. No significant differences in the amounts of other histone modifications in AcH4 (Fig. 8C), AcH3K9 (Fig. 8D) and H3K4me3 (Fig. 8F) were found between AD-LZ and AD-CZ mice. In addition, the DNA methylation frequency at a −820 bp CpG site in the *MT2* promoter of AD-LZ mice was not different from that of the AD-CZ mice (Fig. 8G).

Next, to study the possible involvement of Zn deficiency in the inducibilities of *MT1/2* mRNAs, the Zn-deficient diet was replaced with a regular diet, and the inducibilities of *MT1* and *MT2* mRNAs by Cd administration were examined one month later. Under this condition, no difference in *MT1* and *MT2* mRNA abundances was observed between the AD-LZ and AD-CZ mice 6 h after Cd administration (Fig. 8H). The *MTF1* mRNA abundance was significantly lower in AD-LZ mice than in the AD-CZ mice (Fig. 8I).

Collectively, epigenetic alterations of the *MT2* gene were found to be caused by Zn deficiency during the prenatal period, but not in adulthood.

4. Discussion

A remarkable finding of this study is that epigenetic alterations of the promoter of the *MT2* gene under prenatal Zn deficiency condition are associated with a significant enhancement of Cd-dependent induction of *MT2* mRNA in the liver of mouse progeny later in adulthood. The first question that was addressed is when such epigenetic alterations occur and how long they last. In the 5-week-old

Table 2
Amounts of MTF1 bound to MT2 promoter post Cd administration in the liver of 5-week-old mice born to dams fed a low-Zn diet or a control diet

Target region	Ch-R2			Ch-R3			Ch-R4		
Time post Cd administration (h)	0	1	6	0	1	6	0	1	6
	Fold of enrichment								
IU-CZ	1.00±0.29	9.13±3.44	0.74±0.23	1.00±0.45	6.21±1.60	0.65±0.18	1.00±0.31	3.24±1.08	0.32±0.06
IU-LZ	0.69±0.25	9.17±2.76	0.45±0.10	0.54±0.20	8.00±3.69	1.54±0.25*	0.78±0.19	3.30±1.25	1.16±0.30*

Each target regions are the ones shown in Fig. 5A. Data are expressed as mean±S.E.M. ($n=6$ per group).
Statistically significant difference between IU-CZ and IU-LZ mice by Student's t-test (*$P<.05$).

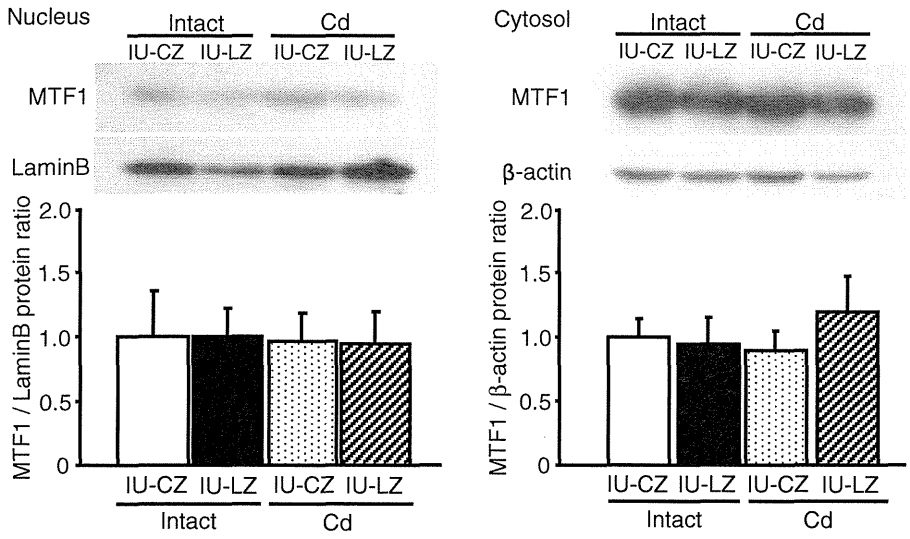

Fig. 7. Amounts of hepatic MTF1 protein in 5-week-old pups grown under Zn deficiency condition. The livers were collected before and 6 h after Cd administration. Scanning densitometry was used for semi quantitative analysis. Data are expressed as mean±S.E.M. (n=5 per group).

IU-LZ mice, significant increases in DNA methylation frequency at the −820 CpG site and histone modifications were demonstrated in comparison with those in IU-CZ mouse progeny. However, this region is not considered to be responsible for transcription. To examine when these histone modifications were caused by Zn deficiency, we analyzed the *MT2* promoter region in the liver from the 1-day-old pups born to dams given a Zn-deficient diet during gestation. Collectively, the IU-LZ mice had significantly elevated AcH3 levels at Ch-R2 and Ch-R3 and showed a tendency of AcH4 levels to increase at Ch-R2 in comparison with IU-CZ mice, suggesting that histone acetylation levels were increased during the prenatal stage. Taken together, zinc deficiency *in utero* alters fetal histone modifications, and these changes are being stored as an epigenetic memory until adulthood (Supplemental Fig. 1). In this study, we could not provide direct evidence on molecular mechanisms by which histone modification enhance Cd-induced *MT2* mRNA expression in IU-LZ mice. However, the elevation in histone acetylation observed in the IU-LZ mice is considered to keep the nucleosome in an "open chromatin" state [38]. Therefore, it is likely that p300 and Sp1 that are known to be recruited by MTF1 [30] will easily make an access to the *MT2* promoter region under the open chromatin condition and that Cd-induced *MT2* mRNA abundance is enhanced in IU-LZ mice. Further studies will be required to reveal the molecular mechanisms how prenatal Zn deficiency regulates not only gene expression via histone modifications, but also maintain histone modifications.

The next question was whether the epigenetic alterations are more specifically induced by Zn deficiency *in utero* rather than in adulthood. When adult mice fed a low-Zn diet (AD-LZ) or those fed a control diet (AD-CZ) were compared, the levels of AcH3/AcH3K14 of the *MT2* gene at Ch-R1 in AD-LZ mice were significantly different from those in AD-CZ mice. However, these changes did not seem to contribute to the alteration of the induction of *MT2* transcription following Cd exposure, because the Ch-R1 region is considered to be irrelevant to transcription (Fig. 4). In addition, the induction of *MT2* mRNA by Cd exposure in AD-LZ mice was not different from that in AD-CZ mice (Fig. 8H). Therefore, it is not likely that the alteration of histone modifications induced by Zn deficiency played a significant role to induce *MT2* mRNA upon Cd exposure in AD-LZ mice. Our results clearly show that mouse fetuses are more responsive to Zn deficiency resulting in epigenetic alterations than adult mice. On the other hand, epigenetic alterations are known to be caused by environmental factors in adulthood as well. Examples of this are an increase in DNA methylation levels of tumor-suppressor genes, such as p16, in the stomach following infection by *Helicobacter pylori* in humans [39,40], DNA hypomethylation of *Pparγ* in mice fed a high-fat diet [41] and DNA hypermethylation of *PPIc* and DNA hypomethylation of *fosB* in nucleus accumbens in cocaine-administered mice [42]. In the case of the nutritional status of Zn, significant epigenetic alterations might occur when adult animals are exposed to extremely low Zn levels for a longer time than under the present experimental conditions.

The other question is how Cd administration enhanced the *MT2* induction in IU-LZ mice compared with IU-CZ mice later in life. A plausible explanation is that the prenatal Zn deficiency induced enhanced histone modifications in the *MT2* promoter region that includes MREs, and that MTF1 or yet-unidentified transcription factors may have easy access to the MRE motif to activate the *MT2* gene expression upon Cd or Zn exposure. This conjecture was supported by the elevated levels of acetylated histones and methylated H3K4 in the *MT2*-400 bp 5′ flanking region in the IU-LZ mice compared with those in the IU-CZ mice (Fig. 5). It is reasonable to think that such an open-chromatin structure persists into adulthood and allows transcription to be activated, as has been reported for other genes such as *Hoxa10* or *Gfap* [43,44].On the other hand, because of the lack of MRE motifs, it is less likely that the change in DNA methylation frequency at −820 bp CpG in the *MT2* promoter region in the IU-LZ mice is associated with the enhanced *MT2* gene expression later in life (Fig. 3).

MTF1 binding to the MRE motif in the *MT1* gene has been proposed to play an important role in the induction of this gene [30]. Although no data are available on the interaction of MTF1 with the *MT2* gene, our reporter gene assay (Fig. 4) and ChIP assay (Table 2) results suggested that MTF1 can bind to the MRE motif in the *MT2* gene. The significantly prolonged MTF1 binding 6 h after Cd administration in the IU-LZ mice (Table 2) may explain the enhanced *MT2* mRNA induction: That is, it is conceivable that the highly acetylated state of histones bound to the DNA fragment adjacent to MREs (Fig. 5) affects the three-dimensional interaction between the MTF1 protein and DNA, and that the net dissociation of MRE with MTF1 may be reduced owing to structural changes in the nucleosome. As described above, the possible removal or slide of histone H3 in *MT1* promoter by Zn treatment may have an interaction with MTF1, and the binding of MTF1 to the promoter is required to initiate the exclusion of histone [45]. Thus, it can be speculated that the

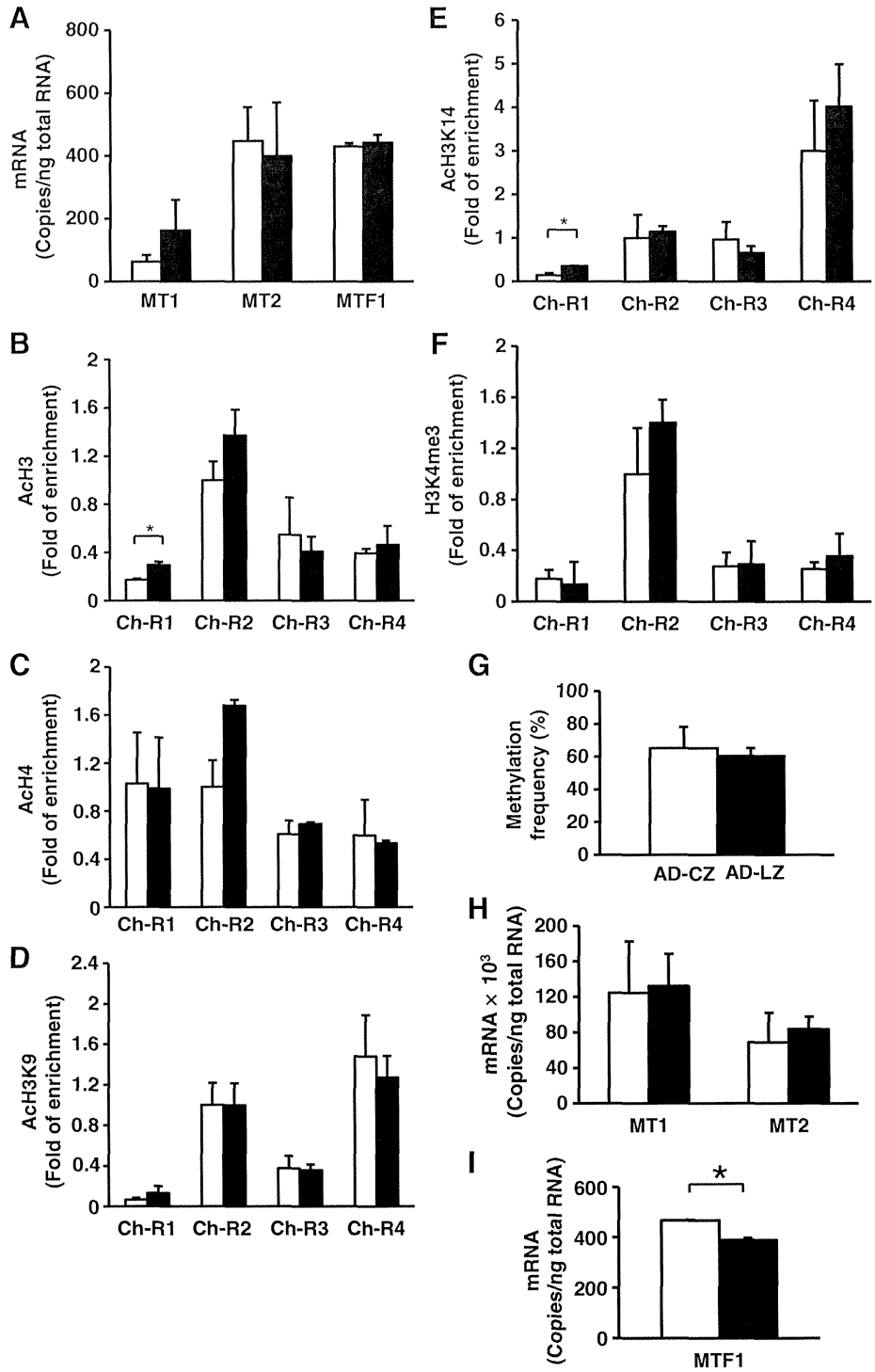

Fig. 8. Abundances of *MT1*, *MT2* and *MTF1* mRNAs, and histone modification in the *MT2* promoter of liver from mice fed a low-Zn diet for 12 days in adulthood (A-G), or those fed with a low-Zn diet followed by a regular diet for a month in adulthood (H-I). (A) *MT1*, *MT2* and *MTF1* mRNAs. (B) Acetylated histone H3. (C) Acetylated histone H4. (D) Acetylated histone H3 lysine 9. (E) Acetylated histone H3 lysine 14. (F) Tri-methylated histone H3 lysine 4. (G) Methylation frequency of −820 bp CpG included in *Aci* I site. See legend to Fig. 5A for target regions of histone modifications. Data on hepatic *MT1* and *MT2* (H) and *MTF1* mRNA (I) were obtained 6 h after oral administration of Cd at 5.0 mg kg^{-1} b.w. Open (AD-CZ mice) and closed (AD-LZ mice) columns are presented. Data are expressed as mean±S.E.M. ($n=3$ per group). Statistically significant difference was determined by Student's t test (*$P<.05$).

prolonged binding of MTF1 to *MT2* promoter in IU-LZ mice may be involved in the maintenance of the opened chromatin structure.

Another question to be addressed is what the enhanced *MT2* mRNA induction in adulthood caused by *in utero* Zn deficiency indicates. It has been reported that abnormal morphogenesis occurred in the *MT1/2*-null fetus grown under Zn deficiency *in utero* [46]. On the contrary, this effect was prevented in the transgenic mice over expressing the MT1 protein [47]. *MT1/2* null mice fed a low-Zn diet for 3 weeks from birth developed swollen Bowman's space in the kidney in comparison with wild-type mice [48]. These studies suggest that MT1/2 proteins protect against Zn deficiency. It can be speculated from our study that mice grown under prenatal Zn deficiency maintain the inducibility of *MT2* mRNA as an epigenetic memory in the genome. In this case, it is thought that mice can be prepared for Zn

deficiency that they may encounter in the future, and that they will be able to efficiently response to the low-Zn condition. This idea could be supported by an analogy to the thrifty phenotype hypothesis in that neonates who experienced poor nutrition *in utero* have metabolic adaptations that emerge in anticipation of a low-quality adult breeding environment [49].

In conclusion, the present study demonstrates for the first time that prenatal Zn deficiency causes epigenetic alterations in the liver of offspring. The enhanced *MT2* gene induction by metal exposure after birth is considered to be due to epigenetic alterations, such as enhanced acetylation levels of histones bound to approximately −400 bp of the *MT2*-5′flanking region. Histone modifications caused by Zn deficiency during the early-developmental period may persist into adulthood as an epigenetic memory. The results of the present study results could also support the DOHaD hypothesis from the perspective that a particular nutrition factor such as an essential trace element during prenatal period can affect epigenome of children.

Acknowledgments

We thank Dr. Chiho Watanabe (Department of Human Ecology, Graduate School of Medicine, The University of Tokyo) for useful suggestions on the result of our experiments, and colleagues in our laboratory for constructive comments.

Appendix A. Supplementary data

Supplementary data to this article can be found online at http://dx.doi.org/10.1016/j.jnutbio.2012.05.013.

References

[1] Painter RC, Roseboom TJ, Bleker OP. Prenatal exposure to the Dutch famine and disease in later life: an overview. Reprod Toxicol 2005;20:345–52.
[2] Barker DJ, Winter PD, Osmond C, Margetts B, Simmonds SJ. Weight in infancy and death from ischaemic heart disease. Lancet 1989;2:577–80.
[3] Barker DJ, Osmond C, Golding J, Kuh D, Wadsworth ME. Growth in utero, blood pressure in childhood and adult life, and mortality from cardiovascular disease. BMJ 1989;298:564–7.
[4] Forsen T, Eriksson JG, Tuomilehto J, Osmond C, Barker DJ. Growth in utero and during childhood among women who develop coronary heart disease: longitudinal study. BMJ 1999;319:1403–7.
[5] Gillman MW, Barker D, Bier D, Cagampang F, Challis J, Fall C, et al. Meeting report on the 3rd International Congress on Developmental Origins of Health and Disease (DOHaD). Pediatr Res 2007;61:625–9.
[6] Torrens C, Poston L, Hanson MA. Transmission of raised blood pressure and endothelial dysfunction to the F2 generation induced by maternal protein restriction in the F0, in the absence of dietary challenge in the F1 generation. Br J Nutr 2008;100:760–6.
[7] Burdge GC, Slater-Jefferies J, Torrens C, Phillips ES, Hanson MA, Lillycrop KA. Dietary protein restriction of pregnant rats in the F0 generation induces altered methylation of hepatic gene promoters in the adult male offspring in the F1 and F2 generations. Br J Nutr 2007;97:435–9.
[8] Simmons RA, Templeton LJ, Gertz SJ. Intrauterine growth retardation leads to the development of type 2 diabetes in the rat. Diabetes 2001;50:2279–86.
[9] Park JH, Stoffers DA, Nicholls RD, Simmons RA. Development of type 2 diabetes following intrauterine growth retardation in rats is associated with progressive epigenetic silencing of Pdx1. J Clin Invest 2008;118:2316–24.
[10] Bernal AJ, Jirtle RL. Epigenomic disruption: the effects of early developmental exposures. Birth Defects Res A Clin Mol Teratol 2010;88:938–44.
[11] Newbold RR, Padilla-Banks E, Jefferson WN, Heindel JJ. Effects of endocrine disruptors on obesity. Int J Androl 2008;31:201–8.
[12] Waterland RA, Travisano M, Tahiliani KG. Diet-induced hypermethylation at agouti viable yellow is not inherited transgenerationally through the female. FASEB J 2007;21:3380–5.
[13] Jones PA, Baylin SB. The fundamental role of epigenetic events in cancer. Nat Rev Genet 2002;3:415–28.
[14] Jenuwein T, Allis CD. Translating the histone code. Science 2001;293:1074–80.
[15] Anway MD, Cupp AS, Uzumcu M, Skinner MK. Epigenetic transgenerational actions of endocrine disruptors and male fertility. Science 2005;308:1466–9.
[16] Tomat AL, Inserra F, Veiras L, Vallone MC, Balaszczuk AM, Costa MA, et al. Moderate zinc restriction during fetal and postnatal growth of rats: effects on adult arterial blood pressure and kidney. Am J Physiol Regul Integr Comp Physiol 2008;295:R543–9.
[17] Halas ES, Eberhardt MJ, Diers MA, Sandstead HH. Learning and memory impairment in adult rats due to severe zinc deficiency during lactation. Physiol Behav 1983;30:371–81.
[18] Halas ES, Hunt CD, Eberhardt MJ. Learning and memory disabilities in young adult rats from mildly zinc deficient dams. Physiol Behav 1986;37:451–8.
[19] Beach RS, Gershwin ME, Hurley LS. Gestational zinc deprivation in mice: persistence of immunodeficiency for three generations. Science 1982;218:469–71.
[20] Tuerk MJ, Fazel N. Zinc deficiency. Curr Opin Gastroenterol 2009;25:136–43.
[21] Vallee BL, Falchuk KH. The biochemical basis of zinc physiology. Physiol Rev 1993;73:79–118.
[22] Hunt JR. Bioavailability of iron, zinc, and other trace minerals from vegetarian diets. Am J Clin Nutr 2003;78:633S–9S.
[23] Wastney ME, Ahmed S, Henkin RI. Changes in regulation of human zinc metabolism with age. Am J Physiol 1992;263:R1162–8.
[24] Menzano E, Carlen PL. Zinc deficiency and corticosteroids in the pathogenesis of alcoholic brain dysfunction — a review. Alcohol Clin Exp Res 1994;18:895–901.
[25] Jeejeebhoy K. Zinc: an essential trace element for parenteral nutrition. Gastroenterology 2009;137:S7–12.
[26] Fischer Walker CL, Ezzati M, Black RE. Global and regional child mortality and burden of disease attributable to zinc deficiency. Eur J Clin Nutr 2009;63:591–7.
[27] Coyle P, Philcox JC, Carey LC, Rofe AM. Metallothionein: the multipurpose protein. Cell Mol Life Sci 2002;59:627–47.
[28] Nies DH. Microbial heavy-metal resistance. Appl Microbiol Biotechnol 1999;51:730–50.
[29] Solis WA, Childs NL, Weedon MN, He L, Nebert DW, Dalton TP. Retrovirally expressed metal response element-binding transcription factor-1 normalizes metallothionein-1 gene expression and protects cells against zinc, but not cadmium, toxicity. Toxicol Appl Pharmacol 2002;178:93–101.
[30] Li Y, Kimura T, Huyck RW, Laity JH, Andrews GK. Zinc-induced formation of a coactivator complex containing the zinc-sensing transcription factor MTF-1, p300/CBP, and Sp1. Mol Cell Biol 2008;28:4275–84.
[31] Vruwink KG, Hurley LS, Gershwin ME, Keen CL. Gestational zinc deficiency amplifies the regulation of metallothionein induction in adult mice. Proc Soc Exp Biol Med 1988;188:30–4.
[32] Tomat AL, Inserra F, Veiras L, Vallone MC, Balaszczuk AM, Costa MA, et al. Moderate zinc restriction during fetal and postnatal growth of rats: effects on adult arterial blood pressure and kidney. Am J Physiol Regul Integr Comp Physiol 2008;295:R543–9.
[33] Wang FD, Bian W, Kong LW, Zhao FJ, Guo JS, Jing NH. Maternal zinc deficiency impairs brain nestin expression in prenatal and postnatal mice. Cell Res 2001;11:135–41.
[34] Oteiza PI, Hurley LS, Lonnerdal B, Keen CL. Marginal zinc deficiency affects maternal brain microtubule assembly in rats. J Nutr 1988;118:735–8.
[35] Shiizaki K, Ohsako S, Koyama T, Nagata R, Yonemoto J, Tohyama C. Lack of CYP1A1 expression is involved in unresponsiveness of the human hepatoma cell line SK-HEP-1 to dioxin. Toxicol Lett 2005;160:22–33.
[36] Clark SJ, Harrison J, Paul CL, Frommer M. High sensitivity mapping of methylated cytosines. Nucleic Acids Res 1994;22:2990–7.
[37] Lee TI, Johnstone SE, Young RA. Chromatin immunoprecipitation and microarray-based analysis of protein location. Nat Protoc 2006;1:729–48.
[38] Kouzarides T. Chromatin modifications and their function. Cell 2007;128:693–705.
[39] Maekita T, Nakazawa K, Mihara M, Nakajima T, Yanaoka K, Iguchi M, et al. High levels of aberrant DNA methylation in Helicobacter pylori-infected gastric mucosae and its possible association with gastric cancer risk. Clin Cancer Res 2006;12:989–95.
[40] Nakajima T, Maekita T, Oda I, Gotoda T, Yamamoto S, Umemura S, et al. Higher methylation levels in gastric mucosae significantly correlate with higher risk of gastric cancers. Cancer Epidemiol Biomarkers Prev 2006;15:2317–21.
[41] Fujiki K, Kano F, Shiota K, Murata M. Expression of the peroxisome proliferator activated receptor gamma gene is repressed by DNA methylation in visceral adipose tissue of mouse models of diabetes. BMC Biol 2009;7:38.
[42] Anier K, Malinovskaja K, Aonurm-Helm A, Zharkovsky A, Kalda A. DNA methylation regulates cocaine-induced behavioral sensitization in mice. Neuropsychopharmacology 2010;35:2450–61.
[43] Bromer JG, Zhou Y, Taylor MB, Doherty L, Taylor HS. Bisphenol-A exposure in utero leads to epigenetic alterations in the developmental programming of uterine estrogen response. FASEB J 2010;24:2273–80.
[44] Asano H, Aonuma M, Sanosaka T, Kohyama J, Namihira M, Nakashima K. Astrocyte differentiation of neural precursor cells is enhanced by retinoic acid through a change in epigenetic modification. Stem Cells 2009;27:2744–52.
[45] Okumura F, Li Y, Itoh N, Nakanishi T, Isobe M, Andrews GK, et al. The zinc-sensing transcription factor MTF-1 mediates zinc-induced epigenetic changes in chromatin of the mouse metallothionein-I promoter. Biochim Biophys Acta 2011;1809:56–62.
[46] Andrews GK, Geiser J. Expression of the mouse metallothionein-I and -II genes provides a reproductive advantage during maternal dietary zinc deficiency. J Nutr 1999;129:1643–8.
[47] Dalton T, Fu K, Palmiter RD, Andrews GK. Transgenic mice that overexpress metallothionein-I resist dietary zinc deficiency. J Nutr 1996;126:825–33.
[48] Kelly EJ, Quaife CJ, Froelick GJ, Palmiter RD. Metallothionein I and II protect against zinc deficiency and zinc toxicity in mice. J Nutr 1996;126:1782–90.
[49] Wells JC. The thrifty phenotype hypothesis: thrifty offspring or thrifty mother? J Theor Biol 2003;221:143–61.
[50] Searle PF, Davison BL, Stuart GW, Wilkie TM, Norstedt G, Palmiter RD. Regulation, linkage, and sequence of mouse metallothionein I and II genes. Mol Cell Biol 1984;4:1221–30.

Research Article

Journal of AppliedToxicology

Received: 1 October 2012, Revised: 4 March 2013, Accepted: 4 March 2013 Published online in Wiley Online Library: 10 June 2013

(wileyonlinelibrary.com) DOI 10.1002/jat.2881

In utero and lactational exposure to 2,3,7,8-tetrachlorodibenzo-*p*-dioxin modulates dysregulation of the lipid metabolism in mouse offspring fed a high-calorie diet

Etsuko Sugai[1], Wataru Yoshioka, Masaki Kakeyama, Seiichiroh Ohsako and Chiharu Tohyama*

ABSTRACT: Exposure to environmental chemicals, including dioxins, is a risk factor for type 2 diabetes mellitus in humans. This study explored the hypothesis that *in utero* and lactational exposure to 2,3,7,8-tetrachlorodibenzo-*p*-dioxin (TCDD), the most toxic congener among dioxins, aggravates this disease state later in adulthood. Pregnant C57Bl/6 J mice were administered either a single oral dose of TCDD (3.0 μg kg^{-1} body weight) or corn oil on gestational day 12.5. The male pups born to these two groups of dams were given either a regular diet or a high-calorie diet, after postnatal day (PND) 28. The four groups of investigated offspring were thus termed T-R (TCDD regular diet), T-H (TCDD high-calorie diet), V-R (vehicle regular diet), and V-H (vehicle high-calorie diet). The mice were regularly monitored for body weight, blood pressure and glucose, until they reached 26 weeks of age. Mice in the V-H group were significantly obese at weeks 15 and 26, but they exhibited no diabetes-associated signs of insulin resistance or hypertension. However, metabolic syndrome-related alterations with marginal signs of liver damage were found at week 26. Pronounced signs of dysregulated lipid metabolism with altered gene expression and liver inflammation were already present at week 15, whereas such alterations were suppressed in the T-H group. Although the mechanism is unclear, this study showed that *in utero* and lactational exposure to low-dose TCDD does not aggravate obesity-induced disease states, such as adult-onset diabetes, but instead attenuates the dysregulation of lipid metabolism brought on by a high-calorie diet. Copyright © 2013 John Wiley & Sons, Ltd.

Keywords: dioxin; environmental chemicals; glucose and lipid metabolism; maternal exposure; mouse

Introduction

The increasing prevalence of diabetes and cardiovascular disease in human populations poses a serious social problem in modern societies. Epidemiological studies suggest that not only intrinsic factors (e.g. obesity-based metabolic alterations), but also extrinsic factors [e.g. exposure to environmental chemicals such as dioxins, polychlorinated biphenyls, and dichlorodiphenyltrichloroethane (DDT)], are associated with the pathogenesis of these disease states (Everett *et al.*, 2007; Fierens *et al.*, 2003; Fujiyoshi *et al.*, 2006; La Merrill *et al.*, 2010). For example, epidemiological studies regarding: (i) Vietnam War veterans previously engaged in the spraying operation of a defoliant containing 2,3,7,8-tetrachlorodibenzo-*p*-dioxin (TCDD) (Michalek *et al.*, 1999); (ii) individuals residing in the vicinity of a polychlorinated biphenyl (PCB)-contaminated Superfund site in the USA (Cranmer *et al.*, 2000); and (iii) workers engaged in handling phenoxy herbicides and chlorophenol (Vena *et al.*, 1998), have all suggested that exposure to environmentally relevant levels of dioxins may be a risk factor for diabetes.

Dioxins are chemicals that are formed unintentionally during combustion. They are persistently and ubiquitously present in the environment and accumulate in various food commodities. TCDD is the most toxic congener among this group of chemicals and induces a variety of toxicities, including carcinogenicity, reproductive and endocrine toxicity, developmental neurotoxicity, and immunotoxicity (van den Berg *et al.*, 2006). Wasting syndrome, characterized by poor weight gain in spite of food intake, weight loss, thymic atrophy and hepatic hypertrophy, is a hallmark of exposure to sublethal doses of dioxin in rodents. Furthermore, exposure to high-dose TCDD alters the energy metabolism (including glucose and lipid metabolism) in rodent livers and cultured cells (Pohjanvirta and Tuomisto, 1994). These toxic events are dependent on the presence of the aryl hydrocarbon receptor (AhR) in affected cells and organs. On the other hand, relatively low doses of TCDD reportedly affect energy metabolism and/or cancer susceptibility. Sato *et al.* (2008) found that C57Bl/6 N mice administered a low daily oral dose of TCDD (5–500 ng kg^{-1} body weight) for 18 days

*Correspondence to: Chiharu Tohyama, Laboratory of Environmental Health Sciences, Center for Disease Biology and Integrative Medicine, Graduate School of Medicine, The University of Tokyo, 7-3-1 Bunkyo-ku, Tokyo, 113-0033, Japan. Email: mtohyama@mail.ecc.u-tokyo.ac.jp

Laboratory of Environmental Health Sciences, Center for Disease Biology and Integrative Medicine, Graduate School of Medicine, The University of Tokyo, 7-3-1 Bunkyo-ku, Tokyo, 113-0033, Japan

[1]Present address: Center for Advanced Biomedical Sciences, Administration and Technology, Management Center for Science and Engineering, Waseda University, 2-2 Wakamatsu-cho, Shinjuku-ku, Tokyo, 162-8480, Japan

developed alterations in the expression of genes associated with energy metabolism in an AhR-dependent manner; hence, AhR apparently mediates actions of both high- and low-dose TCDD. Furthermore, La Merrill *et al.* (2010) administered TCDD (1 $\mu g\,kg^{-1}$ body weight) to pregnant mice on gestational day 12.5, and then fed the offspring either a high-fat diet or a regular diet, and administered 7,12-dimethylbenz[a]anthracene as a cancer initiator. They found that the incidence of breast cancer was significantly increased in the offspring fed a high-fat diet and given the carcinogen. In addition, a plethora of published works have shown that exposure to exogenous conditions *in utero*, such as nutritional factors and certain environmental chemicals, similarly affects the postnatal development of the fetus so as to increase the risk of disease in adulthood (Bernal and Jirtle, 2010; Newbold *et al.*, 2008; Waterland *et al.*, 2007). However, little is understood regarding the underlying mechanism behind: (i) the interaction between diet and *in utero* and/or lactational exposure to low-dose TCDD that goes on to affect; and (ii) the development of metabolic syndrome and altered expression of genes associated with energy metabolism later in life.

In the present study, we hypothesized that *in utero* and lactational exposure of mice to a dose of TCDD that is too low to exert overt maternal or fetal toxicity may affect the glucose metabolism and aggravate diabetes mellitus in adulthood. However, no physiological changes were observed to support this hypothesis during the present 26-week observation period. Coincidently, we found that offspring fed a high-calorie diet developed a dysregulation in lipid metabolism that was apparently attenuated by *in utero*/lactational exposure to TCDD. Therefore, we investigated possible diet-mediated alterations in gene expression related to lipid metabolism and the influence of TCDD on such alterations.

Materials and Methods

Reagents

TCDD (purity, >99.5%), purchased from Cambridge Isotope Laboratories (Andover, MA, USA), was diluted with corn oil (Wako Pure Chemicals Ind., Osaka, Japan) to prepare an ingestion solution. The corn oil containing 2% n-nonane (Nacalai Tesque, Kyoto, Japan) was used as the vehicle. Human insulin (Humalin R; Eli Lily Japan, K.K., Kobe, Japan), SuperScript III reverse transcriptase (Invitrogen, Carlsbad, CA, USA), SYBR Premix Ex Taq (Perfect Real Time, Takara Bio Inc., Otsu, Japan), an RNeasy Mini Kit (Qiagen K.K., Tokyo, Japan) and DNase I (Qiagen K.K.) were purchased from the manufacturers shown in the parentheses. The primers for the real-time reverse-transcription polymerase chain reaction (RT-PCR) were manufactured by Hokkaido System Science Co. (Sapporo, Japan). Unless otherwise indicated, all other chemicals and reagents were of analytical grade and purchased from Wako Pure Chemical Industries and Nacalai Tesque.

Animals and TCDD Exposure

Pregnant C57Bl/6J mice were purchased from CLEA Japan (Tokyo, Japan) and kept under a controlled temperature (23 ± 1 °C) and humidity (50 ± 10%) on a 12/12 h light–dark cycle in an animal facility of the University of Tokyo. The experimental protocols of animal experiments of this study were approved by the Animal Care and Use Committee of the Graduate School of Medicine of the University of Tokyo. These animals received standard mouse chow (Labo MR Stock; Nihon Nosan Kogyo, Yokohama, Japan) or a high-calorie diet (High-calorie 32; CLEA Japan) and water *ad libitum*. One gram of the high-calorie diet contained 5.07 kcal (20.1% protein, 23.2% carbohydrate and 56.7% fat by total kcal) and that of the regular diet contained 2.31 kcal (32.6% protein, 52.2% carbohydrate and 15.2% fat by total kcal). Pregnant mice were administered by gavage TCDD (3.0 $\mu g\,kg^{-1}$ body weight) or corn oil (vehicle) on gestation day (GD) 12.5. This TCDD dosage was selected based on our pilot study result in that no overt maternal or fetal toxicity was induced (data not shown). It has been known that the placental structure of the mouse is developed by 12.5 days of gestation (Malassiné *et al.*, 2003), and this day was selected as the day of dioxin administration. In addition, dioxins administered during gestation have been established to be transferred not only to the fetuses via the placenta, but also to neonates via lactation (Li *et al.*, 1995). Substantial amounts of TCDD were detected in milk remaining in the stomach of newborn pups (Nishimura *et al.*, 2005). All dams were allowed to litter spontaneously. The number of pups per litter was adjusted

Table 1. Primer sequence of genes

Primer	Forward	Reverse
ACOX	AGAGTGGCCTTGACCTCTGA	CCAATGCCACAGACACAGAC
BOX	GCTGCTAAGGCTCACTGCTA	ACGCTGAATCTCTGGTTCGT
Cyclophiln B	TCGGCAAAGTTCTAGAGGGC	TCTGTGGGGATTGACAGG
CYP1A1	GTTACTGGCTCTGGATACCC	GACAATGCTCAATGAGGCTG
CYP1A2	ACTTTGTGGAGAATGTCACCTCAG	TTGAACAGGGCACTTGTGATGTC
CYP4A10	TTTGCCAGAATGGAGAATGG	CTGTTGGTGCTCAGGGTGT
CYP4A14	GACTCTTGGGACAATGGACA	GTTCCTTCCTCTGGCTGGTA
FAS	AGGACTTGGGTGCTGACTACA	TGGATGATGTTGATGATGGA
HADHa	TGACTGCCTGAGTGCCTTG	GGAGTATCTTTCGCATCCTGGTA
LCAD	ATGGCAAAATACTGGGCATC	ACCCGAGCATCCACGTAAG
PPAR-γ2[a]	TTGAGTTTGCTGTGAAGTTCAAT	CAGCAGGTTGTCTTGGATGT
SREBP-1c	GTGGCAAAGGAGGCACTACA	CAGGAGCCGACAGGAAGG.
TNF-α	CACCACCATCAAGGACTCAA	ACAGAGGCAACCTGACCACT

[a]Ogawa *et al.* (2004)

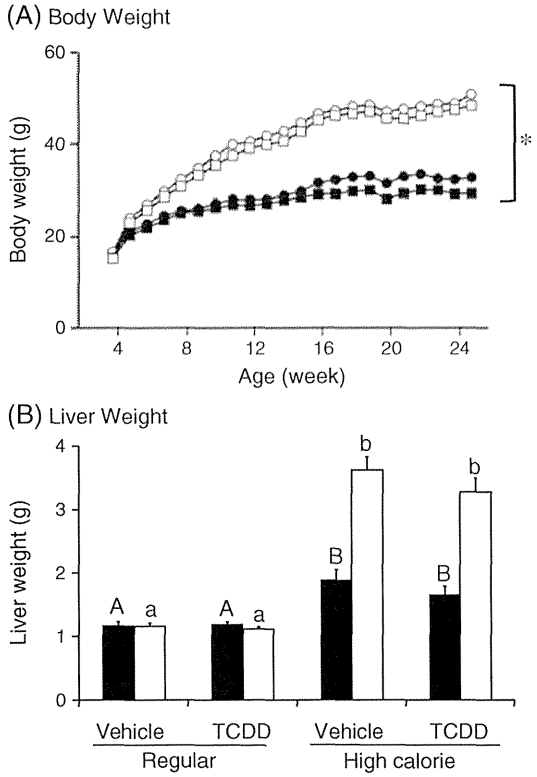

Figure 1. Time courses of body weight (A) and liver weight (B) of mice exposed to 2,3,7,8-tetrachlorodibenzo-*p*-dioxin (TCDD) *in utero* and via lactation, which were fed a regular diet or a high-calorie diet after weaning. Pregnant mice ($n = 9$–10 per group) were administered once by gavage TCDD (3.0 μg kg^{-1} body weight) or corn oil on gestation day (GD) 12.5. The number of litters was adjusted to 6 per dam on postnatal day (PND) 2. From PND 28, male mice were fed either a regular (R) diet or a high-calorie (H) diet, generating four groups ($n = 9$–10 mice per group): (i) vehicle and a regular diet (V-R); (ii) vehicle and a high-calorie diet (V-H); (iii) TCDD and a regular diet (T-R); and (iv) TCDD and a high-calorie diet (T-H). (A) The body weight was significantly different between the high-calorie diet groups (V-H, open circle; T-H, open square) and the regular diet groups (V-R, closed circle; T-R, closed square) from 5 weeks of age, 1 week after feeding the regular or a high-calorie diet by ANOVA with a post hoc test ($P < 0.001$). Asterisks are used to indicate a significant difference of diet. Error bars for each point were too small to be shown in this figure. (B) Liver weight at 15 (closed bar) and 26 (open bar) weeks of age are shown. Differences in the mean of V-R, V-H, T-R and T-H were compared within each age group, and values with different letters (uppercase and lowercase letters for 15 and 26-week-old mice, respectively) indicate a statistically significant difference from each other at $P < 0.05$. No statistical comparison was performed between the V-R and T-H groups, or between the T-R and V-H groups.

to 6 on postnatal day (PND) 2 to minimize the possible effects owing to the litter size. The majority of the pregnant mice delivered 6–11 pups per litter. However, we had pregnant mice that had three to five pups at birth, foster pups from dams that had more than 6 pups at birth and all the pregnant mice nursed a total of 6 pups.

On PND 28, the body weight of male pups born to dams given TCDD or corn oil was measured and the male pups of each treatment group were subdivided into two more groups (regular diet and high-calorie diet). Thus, four groups of pups were used in this study: Group 1 with vehicle and a regular diet (referred to as V-R, thereafter), $n = 20$ from 10 dams; Group 2 with vehicle and a high-calorie diet (V-H), $n = 20$ from 9 dams; Group 3 with TCDD and a regular diet (T-R), $n = 21$ from 8 dams; Group 4 with TCDD and a high-calorie diet (T-H), $n = 22$ from 10 dams.

Monitoring of Health Conditions and Glucose Tolerance and Insulin-resistant Tests

During the experimental period, the body weight and food intake of mice born to dams given vehicle or TCDD were monitored once a week until week 26. Blood pressure was determined using a Blood Pressure Monitor (Model MK-2000ST, Muromachi Kikai Co, Tokyo, Japan) at 9, 19 and 23 weeks after birth.

The glucose tolerance test (GTT) and the insulin resistance test (IRT) were carried out according to methods reported by Terauchi *et al.* (1997), with some modifications. For the GTT, male mice (12 and 20 weeks old) were subjected to fasting for 13 h before the test. They were then injected intraperitoneally (i.p.) with glucose (1.5 mg g^{-1} body weight). Blood was taken from the tail vein at 0, 30, 60, 120 and 180 min after the glucose injection. Blood glucose levels were determined using a Fuji Dri-Chem7000V Veterinary Chemistry Analyzer (Fujifim Medical Co., Tokyo, Japan). For the IRT, male mice (13 and 21 weeks old) were fed *ad libitum* and then subjected to fasting during the test. They were i.p. challenged with human insulin (0.75 mU g^{-1} body weight). Blood was drawn from the tail vein at 0, 30, 60, and 90 min after insulin injection, and blood glucose levels were determined as described above.

Collection of Blood and Liver Tissues

After overnight fasting, 9 and 11–13 mice from each group were autopsied under diethyl ether anesthesia in the 15th and 26th weeks after birth, respectively. Blood was collected from the abdominal vein during autopsy, followed by the separation of serum for blood analyzes, and liver tissues were collected, snap-frozen in liquid nitrogen and stored at −80 °C until gene expression analyzes.

Real-time RT-PCR

For the analysis of gene expression by real-time RT-PCR, six liver tissues were randomly selected from nine 15-week-old and eleven 26-week-old mice. Total RNA was extracted using RNeasy according to the manufacturer's instructions and purified to obtain a DNase I-digested RNA specimen using an RNeasy Mini column. First-strand cDNA synthesis was carried out with the Super Script III First-Strand Synthesis System for real-time RT-PCR. Total RNA samples (1 μg) were denatured for 5 min at 65 °C with 2.5 μM oligo(dT_{20}), primer and reverse-transcribed with 200 U of Superscript III RT, 0.5 mM dNTP mix and 5 mM dithiothreitol for 50 min at 55 °C, and 10 min at 50 °C, followed by a termination reaction for 15 min at 70 °C. The volume of the reaction mixture for reverse transcription was 20 μl. Quantitative RT-PCR analysis was performed using a LightCycler (Roche Diagnostics K.K., Tokyo, Japan) and SYBR Premix Ex Taq (Perfect Real Time) according to the manufacturer's protocol. The primer sets of genes used in the present study are summarized in Table 1. These genes include acetyl-CoA carboxylase (ACC), acyl-CoA oxidase (ACOX), branched-chain acyl-CoA oxidase (BOX), cyclophiln B

Table 2. Blood pressure (mmHg) and heart rate (beats per min) in mice born to dams exposed to 2,3,7,8-tetrachlorodibenzo-*p*-dioxin (TCDD) or vehicle[a]

	Regular diet				High Calorie diet			
Age	Vehicle		TCDD		Vehicle		TCDD	
(Week)	BP (mmHg)	Heart rate (beats per min)	BP (mmHg)	Heart rate (beats per min)	BP (mmHg)	Heart rate (beats per min)	BP (mmHg)	Heart rate (beats per min)
9	100 ± 7	671 ± 28	104 ± 2	713 ± 11	102 ± 1	718 ± 33	99 ± 4	740 ± 4
19	108 ± 5	690 ± 16	109 ± 3	711 ± 6	98 ± 7	706 ± 11	111 ± 5	726 ± 12
23	116 ± 2	707 ± 3	122 ± 3	728 ± 10	125 ± 4	717 ± 8	125 ± 4	729 ± 6

[a]Data were analyzed on a litter-by-litter basis, using two-way ANOVA to analyze the effects of diet and exposure. The number of dams was 6, 7 or 8 per each group. No differences in systolic blood pressure and heart rate were found.

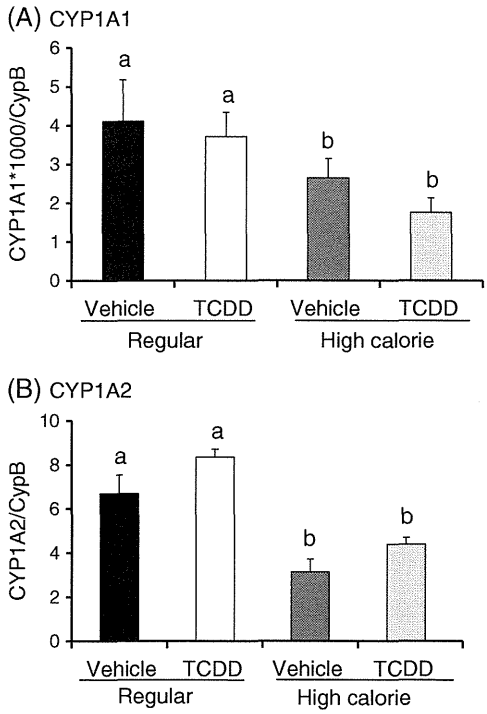

Figure 2. CYP1A1 and CYP1A2 mRNA expression in the liver of 15-week-old mice exposed to 2,3,7,8-tetrachlorodibenzo-*p*-dioxin (TCDD) *in utero* and via lactation, and fed a high-calorie diet or a regular diet after weaning. The group classification is the same as that in Fig. 1. RNA was extracted from the liver. At least one mouse was randomly selected from a litter, and 4–5 litters out of 9 dams were also randomly selected for each group. After the preparation of RNA from the liver, quantitative RT-PCR was performed to determine the CYP1A1 and CYP1A2 mRNA expression levels relative to that of CypB mRNA. Data are shown as the mean ± SE (n = 4–5 per group). No statistical comparison was performed between the V-R and T-H groups, or between the T-R and V-H groups.

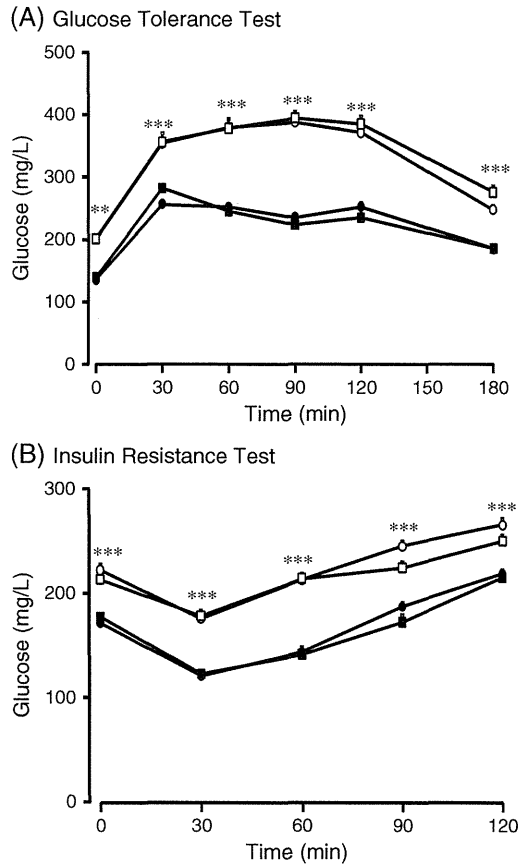

Figure 3. Glucose tolerance test (A) and insulin resistant test (B) in mice exposed to 2,3,7,8-tetrachlorodibenzo-*p*-dioxin (TCDD) *in utero* and via lactation, which were fed a high-calorie diet or a regular diet after weaning. The group classification is the same as that in Fig. 1. The glucose tolerance test and insulin resistance test were performed in 20-week-old mice (n = 7–8 per group) and 21-week-old mice (n = 7–8 per group), respectively. In the both tests, two-way ANOVA with post hoc analysis indicates that there is a significant main effect of diet (P 0.001), but not of exposure, for blood glucose levels, and that they were significantly higher in the high-calorie diet groups (V-H, open circle; T-H, open square) than in the regular diet groups (V-R, closed circle; T-R, closed square). Asterisks indicate a statistically significant difference at $P < 0.01$ (**) and 0.001 (***). No statistical comparison was performed between the V-R and T-H groups, or between the T-R and V-H groups.

(CypB), CYP1A1, CYP4A10, CYPA14, fatty acid synthase (FAS), long-chain acyl-CoA dehydrogenase (LCAD), long-chain L-3-hydroxyacyl-coenzyme A dehydrogenase α (HADHα), peroxisomal proliferator-activated receptor PPAR-γ2, sterol regulatory element-binding protein (SREBP-1c) and tumor necrosis factor TNF-α. The amplification program is described as follows: one cycle of 95 °C for 10 s, followed by 40 cycles of denaturation for 5 s at 95 °C, annealing of primers for 20 s at 60 °C and extension for 15 s at 65 °C. After completion, a melting curve analysis was performed to monitor PCR

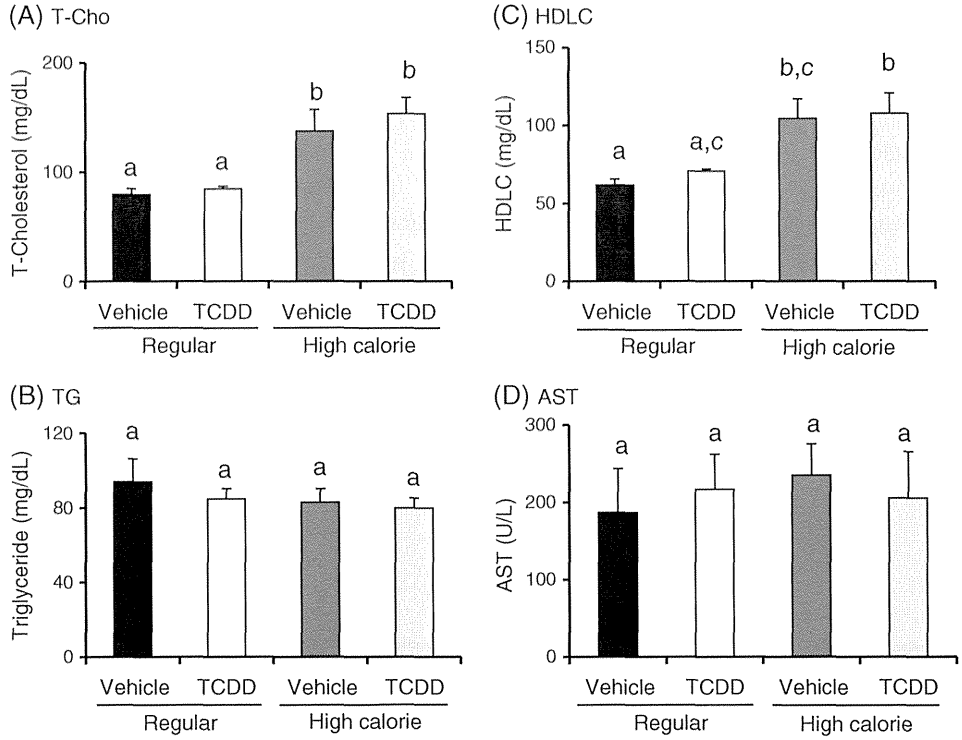

Figure 4. Blood biochemistry of 15-week-old mice, exposed to 2,3,7,8-tetrachlorodibenzo-*p*-dioxin (TCDD) *in utero* and via lactation, that were fed a high-calorie diet or a regular diet after weaning. Total cholesterol (A), triglyceride (B), high-density lipoprotein cholesterol (HDLC) (C) and AST (C) in serum were determined using Fuji Dri-Chem 7000 V. Data are shown as the mean ± SE ($n = 6$–7 per group). Differences in means were analyzed by two-way ANOVA with a post hoc test. Overall, significant main effects of diet were found in (A) and (C). See *P*-values in the 'Results'. No statistical comparison was performed between the V-R and T-H groups, or between the T-R and V-H groups.

product purity. The expression levels of mRNAs of target genes were calculated by the ΔCt method using CypB for normalization.

Statistical Analysis

Data were analyzed on a litter-by-litter basis. SPSS for Windows version 15.0 (SPSS Japan Inc., Tokyo, Japan) was used for the statistical analysis. All data are shown as the mean ± the standard error (SE) of the mean. Differences in means were analyzed by two-way analysis of variance (ANOVA) followed by Tukey's honestly significant difference (HSD) test for post hoc analysis. Unless otherwise stated, no significant interactions between diet (regular diet or high calorie diet) and exposure (dioxin or vehicle) were observed. A *P*-value of less than 0.05 was considered statistically significant.

Results

Body Weight and Blood Pressure

The body weight was not different among the four groups (V-R, V-H, T-R and T-H) at PND 28. The body weight of mouse offspring given a high-calorie diet (V-H and T-H groups) was significantly increased during the entire experimental period (Fig. 1A, $P < 0.05$). A significant main effect of diet at week 15 [$F(1,23) = 16.7$, $P < 0.001$] and at week 26 [$F(1,24) = 214$, $P < 0.001$] was observed on liver weight, but no significant main effect of exposure was observed (Fig. 1B).

No alterations by the type of diet or by TCDD exposure were found for the mean systolic blood pressure at 9, 19 or 23 weeks after birth (Table 2). For example, the systolic blood pressure values (mean ± SE) of 23-week-old mice in the V-R, T-R, V-H and T-H groups were 116 ± 2, 122 ± 2, 125 ± 4 and 125 ± 4 mmHg, respectively. No difference in the pulse rate was found between the groups during the blood pressure measurement.

Effect of TCDD Exposure on CYP1A1 and CYP1A2 mRNA Levels

To examine whether TCDD had direct effects on the mice at 15 weeks of age, mRNA levels of the indicator genes of TCDD exposure, CYP1A1 and 1A2, were measured in the liver (Fig. 2). No significant main effect of exposure was revealed as assessed by CYP1A1 mRNA abundance, but a significant main effect of diet [$F(1,15) = 5.74$, $P < 0.05$] was found by two-way ANOVA. In contrast, CYP1A2 mRNA abundance revealed a significant main effect of exposure [$F(1,15) = 6.48$, $P < 0.05$], as well as a significant main effect of diet [$F(1,15) = 42.9$, $P < 0.001$]. In addition, there was a significant difference between the V-R and V-H groups ($P < 0.001$) and the T-R and T-H groups ($P < 0.001$), whereas no significant differences were observed between the V-R and T-R groups and the V-H and T-H groups. These results suggest that nearly all of the TCDD was eliminated from the body by week 15 after birth, probably owing to the fact that the elimination half-life of TCDD is approximately 11 days in C57Bl/6 mice (Gasiewicz *et al.*, 1983).

Journal of AppliedToxicology

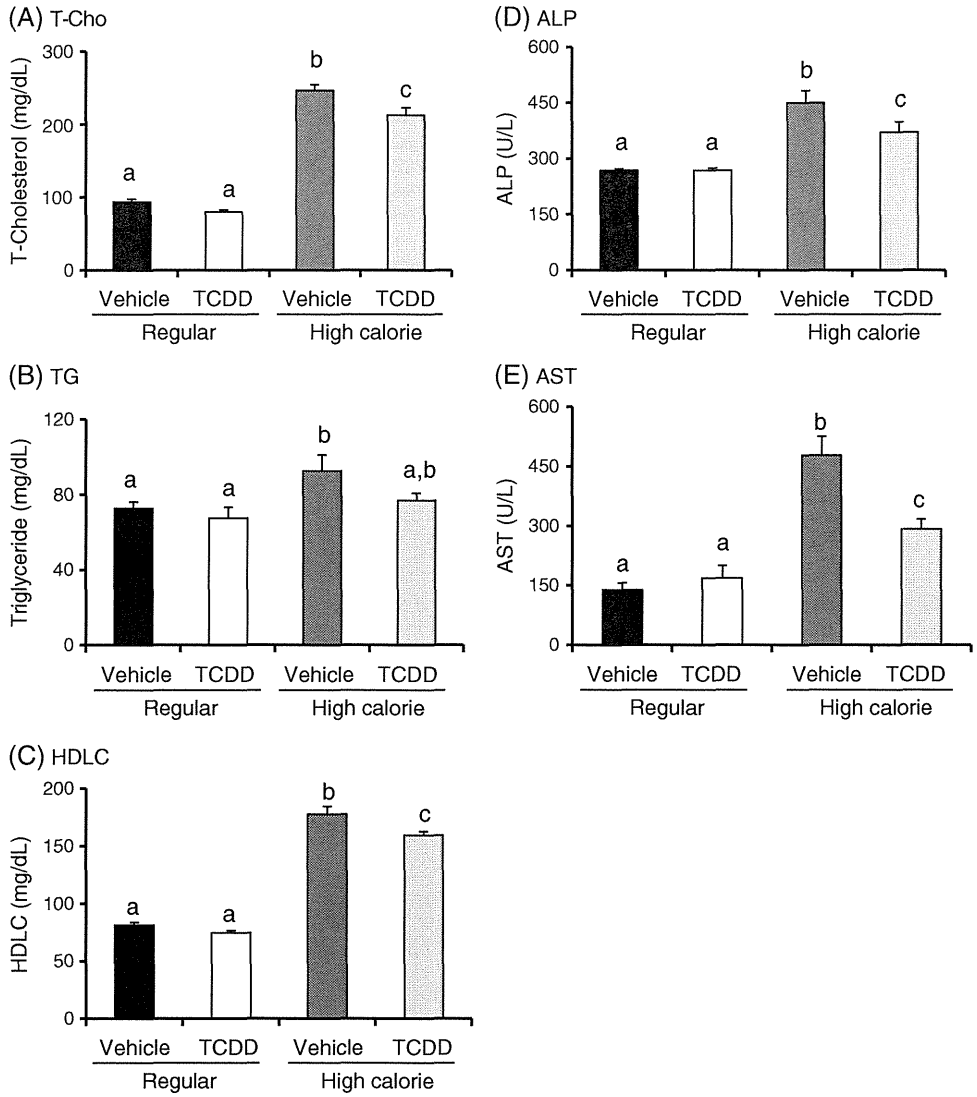

Figure 5. Blood biochemistry of 26-week-old-mice, exposed to 2,3,7,8-tetrachlorodibenzo-*p*-dioxin (TCDD) *in utero* and via lactation, that were fed a high-calorie diet or a regular diet after weaning. Total cholesterol (A), triglyceride (B), high-density lipoprotein cholesterol (HDLC) (C), ALP (D) and AST (E) were determined using Fuji Dri-Chem 7000V. Data are shown as the mean ± SE ($n = 7$ per group). Differences in means were analyzed by two-way ANOVA with a post hoc test. Overall, a significant main effect was observed in (A), (B), (C), (D) and (E) by diet and (A), (C) and (E) by exposure, with a significant interaction in (E). The T-H group was significantly lower than the V-H group in (A), (C), (D) and (E). Values with different letters indicate a significant difference from each other. See *P*-values in the 'Results'. No statistical comparison was performed between the V-R and T-H groups, or between the T-R and V-H groups.

Glucose Tolerance Test (GTT) and Insulin Resistance Test (IRT)

To study the possible effects of *in utero* and lactational exposure to TCDD on glucose metabolism, we carried out the GTT at weeks 12 and 20 after birth and the IRT at weeks 13 and 21 after birth. The significant main effects of diet were observed in the GTT throughout the test period at week 12 [$F(1,156) = 126$, $P < 0.001$] and at week 20 [$F(1,156) = 183$, $P < 0.001$], as shown in Fig. 3A. However, no significant main effect of exposure was found at either of these time points (Fig. 3A).

The significant main effects of diet were also observed in the IRT throughout the test period at week 13 [$F(1,125) = 82$, $P < 0.001$] and at week 21 [$F(1,130) = 181$, $P < 0.001$] (Fig. 3B). However, no significant main effect of exposure was observed (Fig. 3B). The blood glucose concentration in the high-calorie diet groups responded nearly normally to insulin administration, as did the blood glucose concentration in the regular diet groups. This necessitated nullification of our original hypothesis, that *in utero* and lactational exposure to TCDD is involved in the occurrence or aggravation of type 2 diabetes mellitus.

Blood Biochemistry

We examined the blood biochemistry of 15- and 26-week-old mice using two-way ANOVA with the Tukey's HSD post hoc test. At week 15, significant main effects of diet were found on total cholesterol [$F(1,23) = 21.6$, $P < 0.001$] and HDLC levels [$F(1,23) = 16.5$, $P < 0.001$], but no significant main effects of diet

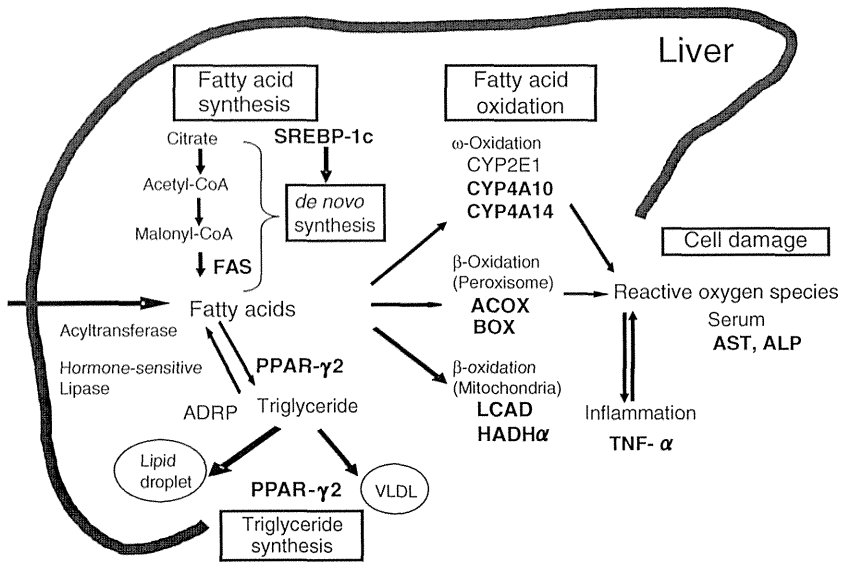

Figure 6. A scheme of fatty acid metabolism in the liver. Genes in the liver and substances in serum analyzed in this study are shown in bold. See abbreviations in text.

or exposure were observed on triglyceride or AST levels (Fig. 4). In contrast, at week 26, comparison of total cholesterol levels yielded significant main effects of exposure [$F(1,26) = 9.78$, $P < 0.01$] and of diet [$F(1, 26) = 353$, $P < 0.001$], with a significant difference between the V-H and T-H groups ($P < 0.01$) (Fig. 5A). A significant main effect of diet was observed on triglyceride levels [$F(1,26) = 5.64$, $P < 0.05$] (Fig. 5B), but no significant main effect of exposure was observed. By contrast, high-density lipoprotein cholesterol (HDLC) levels revealed a significant main effect of both exposure [$F(1,25) = 8.30$, $P < 0.01$] and

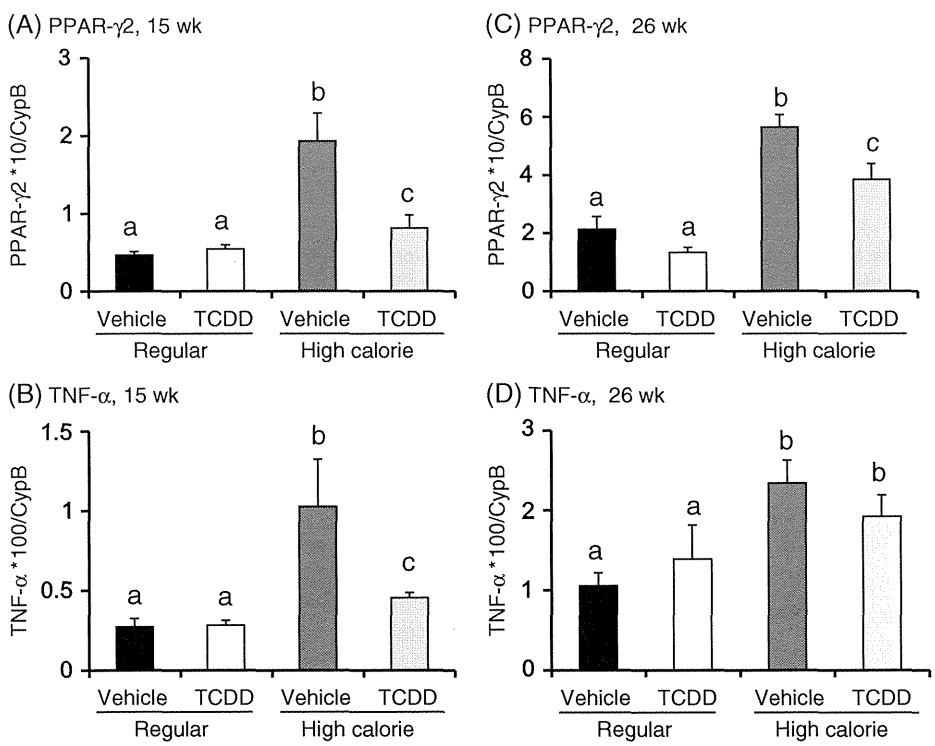

Figure 7. Expression of peroxisomal proliferator-activated receptor PPAR-γ2 (A, C) and tumor necrosis factor TNF-α (B, D) genes in the liver from 15-week old (A, B) and 26-week-old (C, D) mice, exposed to 2,3,7,8-tetrachlorodibenzo-*p*-dioxin (TCDD) *in utero* and via lactation, that were fed a high-calorie diet or a regular diet after weaning. Data are shown as the mean ± SE ($n = 4$–5 per group) after normalization with CypB. Differences in means were analyzed by two-way ANOVA with a post hoc test. Differences in means were analyzed by two-way ANOVA with a post hoc test. Overall, a significant main effect was observed in (A), (B), (C) and (D) by diet, and (A), (B), and (C) by exposure, with a significant interaction in (A) and (C). The T-H group was significantly lower than the V-H group in (A), (B), and (C). Values with different letters indicate a significant difference from each other. See P values in the 'Results'. No statistical comparison was performed between the V-R and T-H groups, or between the T-R and V-H groups.

Journal of AppliedToxicology

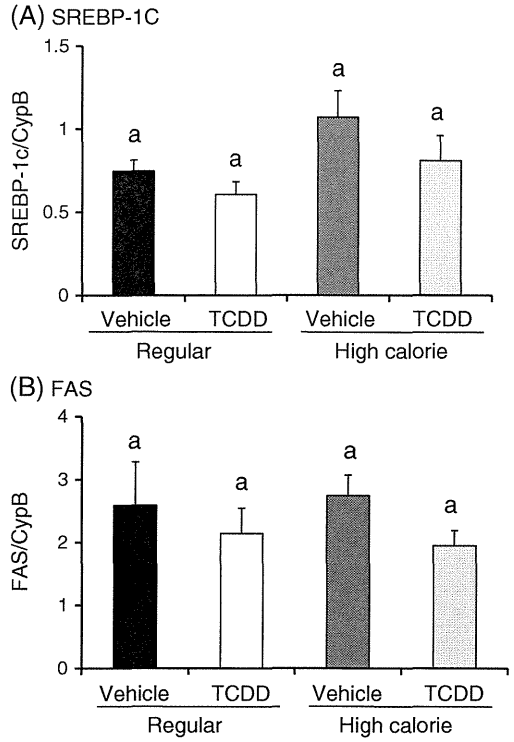

Figure 8. Expressions of SREBP-1c (A) and FAS (B) genes in the liver from 15-week-old mice, exposed to 2,3,7,8-tetrachlorodibenzo-*p*-dioxin (TCDD) *in utero* and via lactation, that were fed a high-calorie diet or a regular diet after weaning. Data are shown as the mean ± SE ($n = 4$–5 per group) after normalization with CypB. Differences in means were analyzed by two-way ANOVA with a post hoc test. Overall, a significant main effect by diet was observed in (A) at $P < 0.05$. No statistical comparison was performed between the V-R and T-H groups, or between the T-R and V-H groups.

of diet [$F(1,25) = 432$, $P < 0.001$], again with a significant difference between the V-H and T-H groups ($P < 0.01$) (Fig. 5C). A significant main effect of diet [$F(1,25) = 35.7$, $P < 0.001$], but not of exposure, was observed on ALP levels, with a significant difference between the V-H and T-H groups ($P < 0.05$) (Fig. 5d), whereas a significant main effect of exposure [$F(1,25) = 5.16$, $P < 0.05$] and of diet [$F(1, 25) = 45.3$, $P < 0.001$] was observed on AST levels, with a significant interaction between diet and exposure [$F(1,25) = 9.77$, $P < 0.01$]. The T-H group was significantly lower than the V-H group ($P < 0.001$) (Fig. 5E).

Lipid Metabolism-related Gene Expression in the Liver

Given our coincidental observation regarding diet-dependent alterations in lipid metabolism, we next investigated how *in utero* and lactational exposure to TCDD affects lipid metabolism-related gene expression (see schematic diagram in Fig. 6). Because the blood biochemistry revealed signs of metabolic syndrome in the high-calorie diet groups at week 15, with marginal signs of liver damage at week 26, we first examined the mRNA expression levels of PPAR-γ2 and TNF-α in the liver at these time periods.

At week 15, the significant main effects of exposure [$F(1,15) = 8.81$, $P < 0.01$) and of diet [$F(1,25) = 24.2$, $P < 0.001$] were observed on PPAR-γ2 mRNA expression levels, with a significant interaction between exposure and diet [$F(1,15) = 11.4$, $P < 0.01$). The V-H group showed a significantly higher expression level of PPAR-γ2 mRNA relative to the V-R group, but the enhanced expression of PPAR-γ2 mRNA was significantly suppressed in the T-H group relative to the V-H group ($P < 0.001$) (Fig. 7A). At week 26, the alterations in mRNA expression levels observed in the liver at week 15 became less marked, but the significant main effects of exposure [$F(1,15) = 7.51$, $P < 0.05$ and of diet [$F(1,15) = 40.8$, $P < 0.001$] were still found, without a significant interaction between the two factors (Fig. 7C). The increased PPAR-γ2 mRNA expression levels continued to be significantly suppressed in the T-H group compared with the V-H group ($P < 0.001$) (Fig. 7C). At week 15, the significant main effects of exposure [$F(1,15) = 4.95$, $P < 0.05$] and of diet [$F(1,15) = 13.5$, $P < 0.01$] were also found on TNF-α mRNA abundance, with a significant interaction between exposure and diet [$F(1,15) = 5.28$, $P < 0.05$]. Like PPAR-γ2 mRNA expression levels, the enhanced TNF-α mRNA expression levels were significantly suppressed in the T-H group versus the V-H group ($P < 0.01$) (Fig. 7B). At week 26, a significant main effect of diet was observed on TNF-α mRNA abundance [$F(1,15) = 7.11$, $P < 0.05$], but no significant difference was observed between the V-H and T-H groups (Fig. 7D).

We then focused on the gene expression of lipid metabolism-related genes in the liver at week 15 (see schematic diagram in Fig. 6). First, we examined the mRNA expression levels of SREBP-1c and FAS, both of which are responsible for the *de novo* synthesis of fatty acids in the liver. A significant main effect of diet [$F(1,15) = 5.08$, $P < 0.05$], but not of exposure, was found on SREBP-1c mRNA abundance (Fig. 8A), whereas no significant main effect of either exposure or diet was observed on FAS mRNA abundance (Fig. 8B).

Next, we determined the mRNA expression levels for genes that are responsible for the β-oxidation of fatty acids, including LCAD, HADHα, ACOX and BOX (Fig. 9). A significant main effect of diet [$F(1,15) = 45.9$, $P < 0.001$), but not of exposure, was observed on LCAD mRNA abundance. The increased LCAD mRNA abundance in the V-H group was significantly attenuated in the T-H group ($P < 0.05$) (Fig. 9A). By contrast, no significant main effect of exposure or of diet was observed on HADHα mRNA abundance (Fig. 9B). A significant main effect of diet [$F(1,15) = 22.3$, $P < 0.001$), but not of exposure, was observed on ACOX mRNA levels, and the increased ACOX mRNA levels in the V-H group were significantly suppressed in the T-H group ($P < 0.05$) (Fig. 9C). Finally, BOX mRNA abundance was subject to a significant main effect of diet [$F(1,15) = 16.6$, $P < 0.001$], but not of exposure, and the increased BOX mRNA abundance in the V-H group was significantly reduced in the T-H group ($P < 0.05$) (Fig. 9D).

The gene expression levels of CYP4A10 and CYP4A14, which take part in ω-oxidation of fatty acids, were next determined. The significant main effects of exposure [$F(1,14) = 4.80$, $P < 0.05$] and of diet [$F(1,25) = 31.2$, $P < 0.001$] were found on CYP4A10 mRNA levels. The increased abundance in the V-H group was significantly suppressed in the T-H group ($P < 0.05$) (Fig. 9E). By contrast, a significant main effect of diet only [$F(1,15) = 32.1$, $P < 0.001$), was observed on CYP4A14 mRNA levels (Fig. 9F).

Discussion

Epidemiological observations on the association between low birth weight and coronary heart disease later in life, was formulated to be a theory on 'developmental origins of health and

